JOURNAL OF APPLIED RESEARCH ON SCIENCE AND TECHNOLOGY

TCI Journal Classification
tier
1
Approved during 2022-2024

INSTITUTE OF RESEARCH AND DEVELOPMENT
RAJAMANGALA UNIVERSITY OF TECHNOLOGY THANYABURI

ISSN Online
2773-9473

Volume 22 Issue 2
May – August 2023

JARST
RMUTT

Journal of Applied Research on Science and Technology (JARST)

E-ISSN : 2773-9473
Vol. 22 No. 2 May - August 2023

The Journal of Applied Research on Science and Technology (JARST) aims to disseminate and share knowledge and ideas in the form of high-quality articles to academia, professionals, industrialists, and an important forum for exchanging knowledge between researchers, academics, faculty members and students both national and international, which will bring benefits in building academic cooperation and network that will lead to sustainable use of research. The articles that will be published in this journal must not be ever presented and published or in the evaluation processes in any other journals. Any piracy occurred will be only under the responsibility of the authors. The journal will not be responsible for such consequences.

Aims and Scope

The scope of the journal includes the following areas of research: General Engineering, General Materials Science, General Agricultural and Biological Sciences, General Computer Science, and General Mathematics with particular emphasis on issues that deepen in the basic and applied research. The JARST includes full length original, novel research articles and review articles. Accepted articles are immediately available online and are freely accessible without any restrictions or any other obligations to researchers and scholarly people globally.

Review Process

1. Evaluation by the Editor-in-Chief

The Editor-in-Chief will see whether the topic and theme of the article are appropriate and congruent with the stipulated objectives and format of the Journal. Plagiarism and benefits relating to theory and business contribution will also be investigated. The submitted paper may be returned to the author for preliminary revising or, if the aforesaid criteria are not met, rejected.

2. Evaluation by Review

All submitted manuscripts must be reviewed by at least two expert reviewers in the related fields. Reviewers will evaluate the quality of submitted article for publication via the double-blinded review system.

3. Evaluates the Reviews

The Editor-in-Chief make decision for article publication based on the external readers' evaluation. The said decision is either accepting the article for publication, rejecting it, or resending it back to the author for further elaborating revision.

Period of Issued Journal

The Journal of Applied Research on Science and Technology (JARST) will be 3 issues/year, as follows:

1st issue: January –April
2nd issue: May – August
3rd issue: September - December

Editorial Board

Arunachala Mada Kannan	Arizona State University, USA
Chaudhery Mustansar Hussain	New Jersey Institute of Technology, USA
Hideto Minami	Kobe University, Japan
Kelvin Huang-Chou Chen	National Pingtung University, Taiwan
Yukiya Kitayama	Osaka Metropolitan University, Japan
Chatthai Kaewtong	Mahasarakham University, Thailand
Daniel Crespy	Vidyasirimedhi Institute of Science and Technology, Thailand
Pakorn Opaprakasit	Sirindhorn International Institute of Technology, Thailand
Warayuth Sajomsang	National Nanotechnology Center, Thailand
Chatchai Ponchio	Rajamangala University of Technology Thanyaburi, Thailand
Jakree Srinonchat	Rajamangala University of Technology Thanyaburi, Thailand
Jaturong Lungkapin	Rajamangala University of Technology Thanyaburi, Thailand
Thammasak Rojviroon	Rajamangala University of Technology Thanyaburi, Thailand

Managing Department

Jittima Singto	Rajamangala University of Technology Thanyaburi, Thailand
Monticha Ruttanapan	Rajamangala University of Technology Thanyaburi, Thailand
Mullika Kongpetsak	Rajamangala University of Technology Thanyaburi, Thailand
Nuthawan Thamawatchakorn	Rajamangala University of Technology Thanyaburi, Thailand
Phakhawan Lunkham	Rajamangala University of Technology Thanyaburi, Thailand
Saranya Suwinai	Rajamangala University of Technology Thanyaburi, Thailand
Thitirat Vijanpon	Rajamangala University of Technology Thanyaburi, Thailand
Wasin Buayang	Rajamangala University of Technology Thanyaburi, Thailand

Contact

Institute of Research and Development, Rajamangala University of Technology Thanyaburi (RMUTT)
39 Moo 1, Klong 6, Khlong Luang Pathum Thani 12110 Thailand
Website: https://ph01.tci-thaijo.org/index.php/rmutt-journal/index
Phone: +66 2 5494492, +66 2 5494681
Fax: +66 2 5494680
Email: jarst@rmutt.ac.th

Editorial Note

The Journal of Applied Research on Science and Technology (JARST) is an academic journal prepared by Institute of Research and Development, Rajamangala University of Technology Thanyaburi (RMUTT). The JARST aims to disseminate and share knowledge and ideas in the form of high-quality articles related General Engineering, General Materials Science, General Agricultural and Biological Sciences, General Computer Science, and General Mathematics to researchers, academics, faculty members and students both national and international.

This journal published four research articles. Each of the research articles presented interesting concepts such as Extraction of natural dye from *Oroxylumb indicum* (L.) Kurz by using different solvents for Thai eri silk dyeing, Smart meter design for energy consumption monitoring of residential premises, Mixed Bootstrap-Marascuilo test for testing equality of means under unequal variancesin a completely randomized design and Further investigation on fixed point theorems via C-class functions in extended b-metric spaces. Therefore, this journal is a channel disseminating the knowledge areas of physical sciences and life sciences which related persons could apply it for further benefits.

Lastly, the editorial team would like to considerably thank you for supporting and pushing forward this journal to occur and well accomplish. We are hopeful of your good cooperation and continuing support in the future.

Editorial Team

Contents

Research Articles

Received: January 6, 2023 | Revised: March 9, 2023 | Accepted: March 14, 2023

JARST
JOURNAL OF APPLIED RESEARCH ON SCIENCE AND TECHNOLOGY
INSTITUTE OF RESEARCH AND DEVELOPMENT
RAJAMANGALA UNIVERSITY OF TECHNOLOGY THANYABURI
ISSN ONLINE: 2773-9473
https://ph01.tci-thaijo.org/index.php/
rmutt-journal

Extraction of natural dye from *Oroxylumb indicum* (L.) Kurz by using different solvents for Thai eri silk dyeing

Aritart Sanai*, Thippawan Nachai and Kesorn Merat
Department of Science and Technology, Faculty of Liberal Arts and Science, Roi Et Rajabhat University, Roi Et 45120, THAILAND
*Corresponding author e-mail: Sanaichem@gmail.com

ABSTRACT

Among various textile types in Thailand, silk is the largest market share. Thus, upgrading or developing either the dying process or the quality of fabric dried for Thai silk is still necessary. Natural dyes have become an interesting resource because they are more environmentally friendly than synthetic dyes. Thus, this work aims to study the effect of different solvents for dye extraction from *Oroxylumb Indicum (L.) Kurz* on Eri Thai silk dyeing. Each solvent used for extraction gave a different relative tannic acid and quercetin content. Therefore, this further leads to different properties of dyed fabrics, such as color properties and washing fastness index. From the different solvents studied, the yield of the extracted dyes was on the order of EtOH/water (50: 50) > MeOH/water (50:50) > MeOH ~ EtOH > water. Then, the optimal ratios between EtOH and water in the efficient extraction were varied as follows water, EtOH/water (25: 75), EtOH/water (50: 50), EtOH/water (75:25), and EtOH. The result showed that EtOH/water (50: 50) was still the most effective for dye extraction. In addition, the effect of dose, temperature, and time of *Oroxylumb Indicum (L.)* Kurz was 8.0 g/L, 60 °C, and 60 min, which were considered optimal extraction conditions due to the high relative contents of tannic acid and quercetin. As a result, the fabric of Eri silk dyed has a high quality of fastness rating. Overall, these results could point out the use of extracted dye from *Oroxylumb Indicum (L.) Kurz* has the potential as an alternative dye for Eri Thai silk dyeing.

Keywords: Oroxylum Indicum (L.) Kurz, Ethanol, Water, Natural dye extraction, Eri silk dyeing

INTRODUCTION

Thailand's textile market was valued at USD 8085.0 Billion in 2020 and is projected to reach USD 11097.9 Billion by 2028, growing at a compound annual growth rate (CAGR) of 4.14 % from 2021 to 2028. Among various material types, silk is the largest share of the market [1]. As well as, Thailand is known for its silk, though silk is mainly used for apparel [2]. Thus, upgrading or developing either the dying process or the quality of fabric dried for Thai silk is still necessary.

In general, the majority of the basic ingredients used to color fabrics are synthetic dyes, which take a very long time to degrade [3, 4]. Water has been polluted as a result, and the situation has turned into wastewater. Due to the significant amount of organic debris, the outcome might result in a rise in temperature, a strong stench, a color change, and the demise of aquatic life. A shortage of oxygen may also inhibit the activity of some bacteria [3, 5].

People are becoming increasingly interested in natural textile dyes to reduce the issues above since they degrade faster and are safer than synthetic colors [6]. Additionally, natural dyes offer a variety of lovely hues. As well as, Thailand has a wide variety of plants with great potential for producing natural colors.

One should consider that textiles dyed from natural dyes may have fading problems and low resistance to light and convulsions [6]. Thus, some compounds including potassium dichromate, stannous chloride, stannic chloride, ferrous sulfate, cupric sulfate, and aluminum sulfate are used as dyeing agents to make stronger fibers with the dye [7]. These compounds could generate an affinity (electron acceptors) between the dye and fiber with the

DOI: 10.60101/jarst.2023.251099

coordinate covalent bonds [8, 9]. However, metallic ions of mordants make them insoluble in water and copper, cobalt, chromium, and lead is not considered environmentally friendly when leached into the environment [10].

To overcome the drawback and deal with a more green chemistry issue, this work discloses the use of available natural dyes and mordants such as tannic acid and quercetin extracted from *Oroxylum Indicum (L.) Kurz* for dying silk [10, 11]. These compounds contain a lot of many oxygen atoms and hydroxyl phenolic groups, which could facilitate the creation of hydrogen bonds and/or electrostatic interactions with the fiber, resulting in a good fixation of the dye on the fabric. This remark is possible because the protein and polyamide fibers generate cationic sites in water under acidic conditions resulting in available acid dye anions combining through hydrogen bonding or electrostatic interactions [11, 12]. Besides, *Oroxylumb Indicum* (L.) *Kurz* has been reported as an abundant compound of tannic and alginic acids extracted by water as a solvent [10]. One should be realized that the extraction efficiency of these compounds depends on the kind of solvent system [13]. The solvents with high polarity such as water, methanol, and ethanol would be a good choice for dye extraction containing abundant phenolic group from *Oroxylumb Indicum* (L.) *Kurz* [14]. To our knowledge, there are no reports on the gathering effect of various solvents on the extraction of natural dyes and mordants from *Oroxylum Indicum (L.) Kurz.* Besides, it has no commercial value, plentiful in Thailand. Overall, it is worth investigating as an alternative raw material for natural mordant and dye extraction.

Hence, this work aims to investigate the effect of several solvents, including ethanol, methanol, water, ethanol-water, and methanol-water, for extracting natural dyes from *Oroxylum Indicum (L.) Kurz* on the dying process. Moreover, some properties of fabric dyed, including color characteristics and color fastness relating to washing, are also discussed.

MATERIALS AND METHODS

Materials and Chemicals

Eri silk yarn purchased from the local market of Koh keao Subdistrict, Selaphum District, Roi-Et, Thailand, was used in the present investigation. *Oroxylum Indicum* (L.) bark was from the local area of Roi-Et Rajabhat University, Koh keao Subdistrict, Selaphum District, Roi-Et, Thailand. In order to obtain natural mordants, *Oroxylum Indicum (L.)* bark was extracted by five solvents such as ethanol, methanol, water, ethanol-water, and methanol-water.

Chemicals used in this work were methanol (Lab grade, 99.80% Min) and ethanol (Lab grade, 99.0% Min) were purchased from Giant Leo Intertrade Co.,Ltd., Thailand. Laboratory reagent (LR) grade sodium carbonate obtained from Sigma-Aldrich, and anionic wetting agent (T R Oil, i.e., sulphonated castor oil), non-ionic detergent of the commercial-grade obtained from the local market was used in this investigation.

Degumming of silk

Degumming of silk yarn was performed in a solution containing sodium carbonate or soda ash (0.5 g/L) and non-ionic detergent (2 g/L) at 50 °C for 30 min keeping the material to liquor ratio at 1:30. The degummed yarn was thoroughly washed with cold water and dried at room temperature before dyeing.

Extraction of natural dyes

Oroxylum Indicum (L.) bark was peeled and chopped into small pieces, dried in a dry place for 3 - 5 days, and then thoroughly fine blended with a steel blade. An aqueous solution of *Oroxylum Indicum (L.) bark* of 0.2 g was added with 10 mL of water. The mixture was stirred, heated, and kept at 60 °C for 60 min in a round bottle flask (50.00 mL) connected to a condenser. Finally, it was filtered through a Whatman® Grade 1 filter paper. The filtrate was used for dyeing after diluting with 100 mL of water. Other solvents such as methanol, ethanol, methanol: water (1: 1), and ethanol: water (1: 1) were carried out with the same procedure mentioned above. Moreover, the appropriate concentration of extracted powder from *Oroxylum Indicum (L.)* bark was studied in the range of 0.1, 0.2, 0.4, 0.6, 0.8, 1.0 , and 1.2 g in 10 mL of water. The appropriate time for extraction was determined by varying in the range of 20, 40, 60, 80, and 100 minutes, as well as the optimum result of extraction temperatures was performed at 30, 40, 50, 60, 70, and 80 °C.

To determine the relative content of natural dyes extracted from *Oroxylum Indicum (L.)*, all samples were measured by UV-Visible spectrometer, Hitachi modeled UH5300, at wavelengths of 200 - 800

DOI: 10.60101/jarst.2023.251099

nm. Before the measurement, the extracted dyes were diluted the volume 100 times with DI water.

Moreover, the functional group of extracted dye was determined by Fourier transform infrared spectroscopy (FTIR) a PerkinElmer Spectrum™ 10 with ATR mode in the range from 3500 to 550 cm^{-1} with a resolution of 2 cm^{-1}.

Eri silk dyeing

The pre-mordanting of Eri silk thread was adapted from the method in the literature [10]. A sorbent (aqueous solution of soap or wetting agent) of 1.0 g was diluted in 500 ml of water. The solution was stirred homogeneously to wash the thread of Eri silk. The sample was soaked in the solution for 30 min at 100 °C. Finally, the thread of Eri silk was dried at room temperature for 24 h. For dyeing processes, dye baths were prepared according to the method in the literature [11] and the dyeing was performed without the addition of metal salts. Each treatment sample (1.0000 g of Eri silk) was soaked in various concentrations of prepared natural mordants with a mass ratio of 1:10 based on the Eri silk weight to a natural mordant solution at 60 °C for 1 h (flipped the treatment every 10 min for the whole performance). The pH of the dyeing solution was around 5. Dyed Eri silk was washed with 1.0 g/L of neutral detergent in distilled water for 10 min at 30 °C to eliminate excusably natural mordants. After this, the dyed Eri silk was washed in running water and dried at 40 °C for 30 min. Twice repetitions were performed for each dyed Eri silk using various extracted solvents at the optimum condition of dyed extraction.

Evaluation of color characteristics

X-Rite Colorimetric analysis was used to measure the CIE L*a*b* values. The operating conditions of the equipment were scanning from 200 to 800 nm, Hunter Lab, modeled MiniScan EZ, and observer angle of 10°. CIE L*a*b* values were analyzed by Analysis of Variance (ANOVA) with a 95% confidence interval and multiple comparisons among means (Tukey's tests). L* is a measure of the lightness/darkness of the dyed Eri silk, which ranges from 100 (white) to 0 (black); a* is a measure of the redness/greenness of the dyed Eri silk, with positive (+) values indicating red and negative (-) values green; and b* is a measure of the yellowness/blueness of the dyed Eri silk, with positive (+) values yellow indicating and negative (-) values blue. The greater the magnitude of the* and b* values, the deeper the colors.

Wash fastness characteristics

The detergent (5.0 g) was dissolved in DI water (1000 mL). Each dyed silk piece was treated in the prepared detergent solution (the weight ratio of dyed silk to the detergent solution, 1:50) at 40 °C for 30 min. The sample was washed with DI water three times and dried at room temperature for 24 h. Then, the wash fastness of the dyed silk samples was measured in Launder-o-meter as per the ISO 105-C06:1994 specifications following the literature [15].

Moreover, to ease understanding, the flowchart of the dye extraction process and optimization is summarized in Scheme 1.

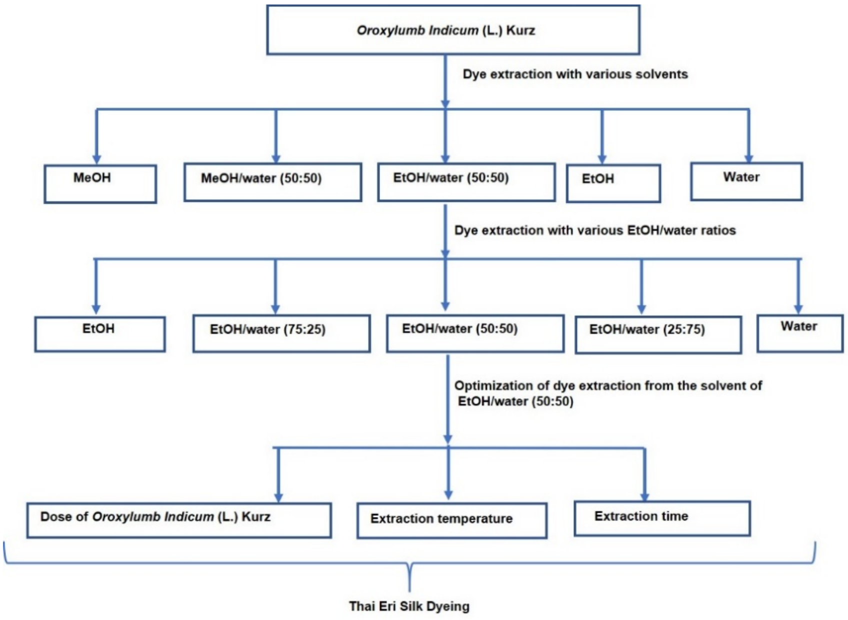

Scheme 1. Diagram of the dye extraction process and optimization in this work.

DOI: 10.60101/jarst.2023.251099

RESULTS AND DISCUSSIONS

Physicochemical properties of extracted dye

Figure 1 demonstrates the UV-Vis spectra of natural mordants extracted from *Oroxylum Indicum (L.)* by various solvents. Three crucial bands at 216, 274, and 330 nm corresponded to the characteristic absorptions of castalagin, tannic acid, and quercetin, respectively [11, 16, 17]. This work focuses on tannic acid and quercetin compounds at the wavelengths of 274 and 330 nm because they behave as both natural dyes and mordants for textile dyeing [11]. The chemical structures of both tannic acid and quercetin, containing mainly a type of polyphenol, are demonstrated in Figure 2. The water solubility of both tannic acid and quercetin is 250 g/L and 0.0215 g/L, but the ethanol solubility of both compounds is 100 g/L and 17 g/L, respectively [18].

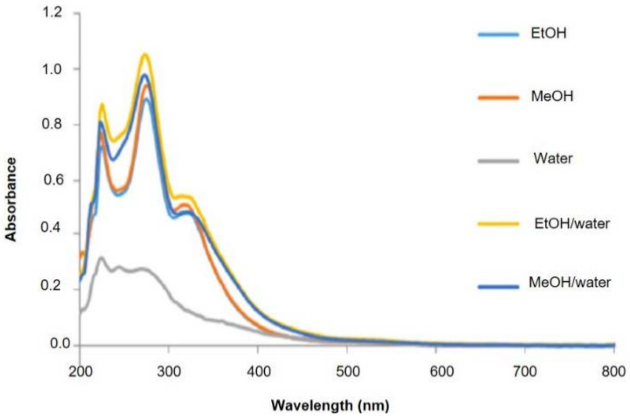

Figure 1 The relationship between absorbance and wavelength of the natural mordants extracted from *Oroxylum Indicum (L.)* bark in different solvents extracted at 60 °C for 60 min.

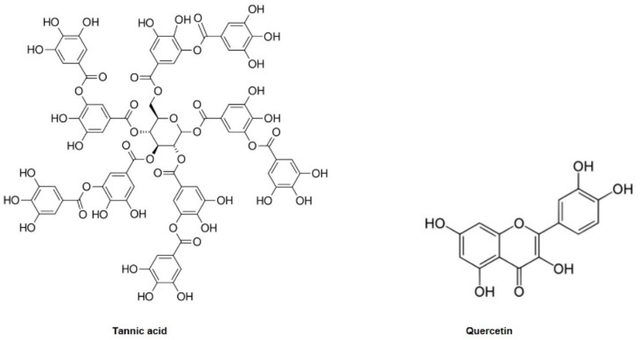

Figure 2 Chemical structures of tannic acid and quercetin.

Moreover, it was noticed that the different solvents used for the extraction provided distinct maxima absorption intensities in the following order EtOH/water (50:50) > MeOH/water (50:50) > MeOH ~ EtOH > water. This result indicates that the co-solvent of EtOH and the water seems the most suitable system for natural mordant extraction.

Figure 3 exhibits FTIR spectra of dye powder extracted using a co-solvent of EtOH/water (50:50). It was observed that there were eleven crucial peaks corresponding to the characteristic functional groups of both tannic acid and quercetin compounds [19, 20]. The bands at 687, 778, and 864 cm^{-1} attributed to =C-H vibrations of arene conjugated to the olefinic group. While the bands at 1048, 1251, 1378, and 1612 cm^{-1} contributed to the vibrations of C-O stretching, C-O-C aryl ketone stretching, C-OH stretching of phenolic hydroxyl group, and C-C stretching of an aromatic ring. Moreover, the bands at 1726, 2172, and 2926 cm^{-1} corresponded to the vibrations of C=O stretching of carboxylate, C-O stretching and C-H stretching, respectively. The broad band at 3219 cm^{-1} was attributed to the vibration of the O-H phenolic hydroxyl group [19, 20]. These character vibrations confirm the presence of both tannic acid and quercetin compounds in the extracted dye from *Oroxylum Indicum (L.)* bark, consistent with UV-Vis results.

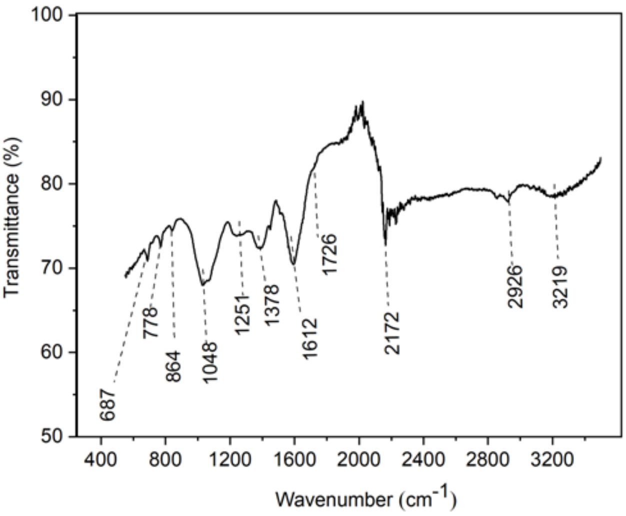

Figure 3 FTIR spectra of dye powder extracted by using a co-solvent of EtOH/water (50:50) at 60 °C for 60 min.

Thus, the co-solvent of water and EtOH system was further selected to optimize extraction capacity with various volume (%) ratios, as illustrated in Figure 4. It was remarked that the extraction efficiency improved with the increase of EtOH content and reached the maximum value at the ratio of 50:50. Then, the decrease in the extraction efficiency was observed with the ratios of 75: 25 and

DOI: 10.60101/jarst.2023.251099

99% ethanol, respectively. This result suggests that the co-solvent with a ratio of 50:50 is the most suitable condition. The consequence might cause by tuning of suitable polarity promoting the extraction efficiency. One should note that tannic acid content is more significant than quercetin in Oroxylum Indicum (L.) bark extraction. This is not much surprising because tannic acid is one of the main components in Oroxylum Indicum (L.) bark [21]. Moreover, the solubility in water and ethanol of tannic acid is more excellent than that of quercetin resulting in better extraction efficiency.

Besides, It was noticed that maxima absorption intensities of EtOH/water (50:50) than other solvents was probably due to water content in the solvent promoting the swelling of *Oroxylum Indicum (L.) bark* pieces. The consequence could increase the contact area between the plant matrix and the solvent, thereby enhancing the extraction yield. Moreover, this result is consistent with the report by Wettasinghe and Shahidi [22] that the co-solvents of water-ethanol (50:50) provide the highest extraction efficiency of flavonoid compounds from *Borago officinalis L.* seeds.

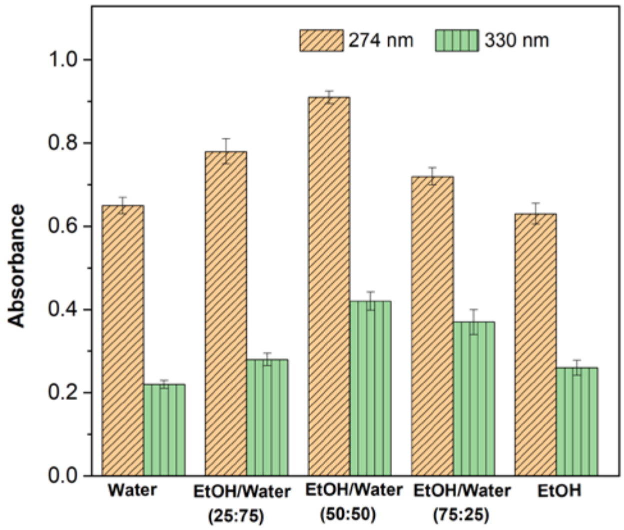

Figure 4 Absorbance of tannic acid and ellagic acid by various water/ethanol ratios at λ (nm) of 274 and 330 nm extracted at 60 °C for 60 min.

Effects of dose, temperature, and time on color intensity for Oroxylum Indicum (L.) bark extraction.

Figure 5 reveals the effect of *Oroxylum Indicum (L.) bark* dose on the obtained color intensity. The color intensity is significantly enhanced with an increase in *Oroxylum Indicum (L.)* bark powder from 2.0 to 8.0 g/L but almost unchanged when the concentration became 10 g/L and 12 g/L. Thus, the optimum concentration for tannic acid and quercetin extraction from *Oroxylum Indicum (L.)* bark was considered for 8 g/L with absorbance values of 0.83 and 0.31 due to the economic aspect.

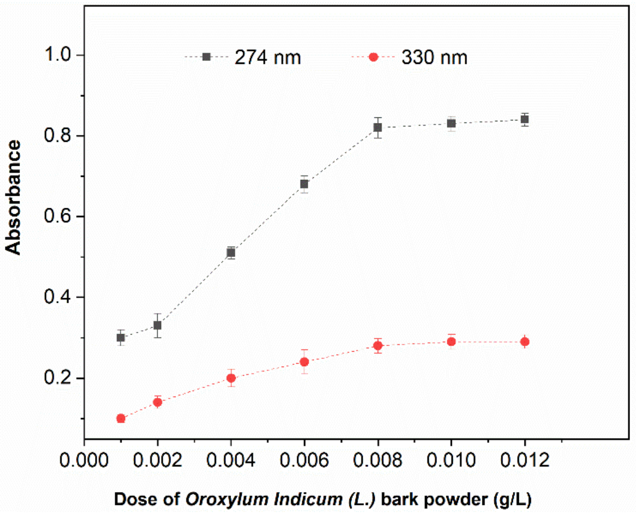

Figure 5 The effect of *Oroxylum Indicum (L.)* bark dose on the color intensity: Extraction condition, a co-solvent of EtOH/water (50:50) at 60 °C for 60 min.

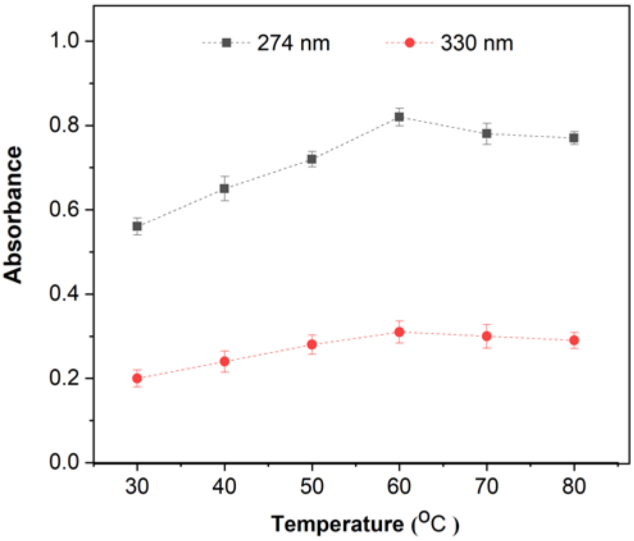

Figure 6 Effects of temperature on color intensity for *Oroxylum Indicum (L.)* bark extraction: Extracted by a co-solvent of EtOH/water (50:50) at various temperatures for 60 min.

Figure 6 displays the effect of extraction temperature on color intensity. The color intensity was dramatically improved with the temperature, from 30 °C to 60 °C. Then, the tendency slightly dropped when the temperature reached 70 °C and

DOI: 10.60101/jarst.2023.251099

80 °C, respectively. Such a decrease in color intensity of these temperatures could result from the slightly lower ethanol concentration in the liquid phase due to the vaporization effect [23]. The assumption is possible because high temperatures, namely, 70 °C and 80 °C, are close and reach the boiling point of ethanol. Thus, the vapor phase of the ethanol becomes dominant in the empty space of the round bottle flask and condenser. The consequence could slightly decrease the ethanol concentration in the liquid phase, consistent with the reported in the literature [23].

Therefore, 60 °C was considered the optimum temperature for further study.

Figure 7 exhibits the effect of extraction time on color intensity. The color intensity was coherently increased with the prolonged extraction time from 20 min to 60 min and became almost constant with times of 70 min and 100 min, respectively. This result suggests that an extraction time of 60 min is the most suitable for optimum conditions. This observation also agrees with the report by Soares and coworkers [23] that the prolonged extraction time could promote the extracted pigments capacity due to greater contact between pigments and solvent, easing the extraction process. Meanwhile, the color intensity decreased after the extraction time. Longer than 60 min may cause by pigment degradation.

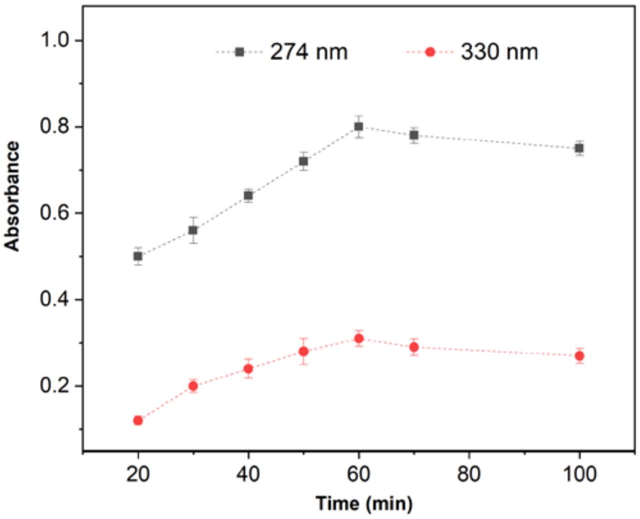

Figure 7 Effects of time on color intensity for *Oroxylum Indicum (L.)* bark extraction: Extracted by a co-solvent of EtOH/water (50:50) with the dose of 8.0 g/L at 60 °C for various times.

Color characteristics of dyed silk

To fairly compare the extracted efficiency based on the solvent effect, the optimum condition for dye extraction in each solvent was a dose concentration of 0.008 g/L, a temperature of 60 °C, and a time of 60 min. Then, the Eri silk was dyed in each solvent with the method adapted from the literature [11].

Figure 8 demonstrates the color appearance of dyed Eri silk with various solvents. The Non-dyed Eri silk had a white color, but the colors of the fabrics dyed became stronger; light yellow (water), yellowish green (EtOH/water, 25:75), dark green (EtOH/water, 50:50), Dark green (EtOH/water, 75: 25), and yellowish dark green (EtOH). The color strength of dyed Eri silk seemed consistent with the increase in the relative content of tannic acid and quercetin compounds [11]. Moreover, different extracted solvents could result in distinct dyed adsorption efficiencies (%) of the fabrics, as illustrated in Table 1. The result showed that the extracted dye with EtOH /water (50: 50) gave the highest adsorption efficiency. Meanwhile, a drastic drop in adsorption was observed in the solvents of EtOH/water (75: 25) and EtOH. This phenomenon is probably due to the more favorable dissolution of tannic acid and quercetin compounds in the ethanol layer rather than the interaction with silk.

Figure 8 Color appearance of dyed Eri silk fabrics in various solvents; (1) non-dyed Eri silk fabrics (2) water, (3) EtOH/water (25: 75), (4) EtOH /water (50: 50), (5) EtOH /water (75: 25), and (6) EtOH.

Table 1 Absorption efficiency (%) comparing pre-dyeing and post-dyeing with various kinds of solvents.

λ_{max} (nm)	Solvent	^{a}Absorption efficiency (%)
274	Water	42.1
	EtOH/Water (25:75)	45.9

DOI: 10.60101/jarst.2023.251099

λ_{max} (nm)	Solvent	[a]Absorption efficiency (%)
	EtOH/Water (50:50)	56.7
	EtOH/Water (75:25)	14.6
	EtOH	14.9
330	Water	40.1
	EtOH/Water (25:75)	46.8
	EtOH/Water (50:50)	57.5
	EtOH/Water (75:25)	15.4
	EtOH	16.3

[a] Calculated by the following equation = (absorption intensity of pre-dyeing - absorption intensity of post-dyeing / absorption intensity of pre-dyeing) × 100

Furthermore, the color data values have altered in the presence of several solvents used in the extraction, as displayed in Table 2. It was found that water-dyed-silk provided the highest L^* value of 76.9, indicating a brighter color than ethanol and a mixture of ethanol/water-dyed-silks [11]. All solvents-dyed-silks gave relatively low values of a^* ranging from -1.69 to 1.93, suggesting a dominant greenness. While b^* values in the range of 26.49 - 17.90 were observed from the silks dyed with water, a mixture of ethanol/water, and ethanol, convincing yellowness [24]. Overall, these results correlate well with the appearance of colors observed by the naked eye.

Colorfastness to washing dyed silks (at 40 °C following ISO 105-C06:1994) from various extraction solvents is demonstrated in Table 3. The fastness rating of the samples dyed with several extracted dye solvents provided slightly different fastness qualities. Silk fabrics dyed with the extracted solvents of water, EtOH/Water (25:75), and EtOH/Water (50:50) were very good fastness ratings (4-5). In terms of silk fabrics dyed with the extracted solvents of EtOH/Water (50:50) and EtOH gave fair to good (3-4) and fair (3), respectively. The greater fastness ratings of silk fabrics dyed with the extracted solvents containing high water content might cause by better absorption efficiency (Table 1). The assumption is rational because flavonoid-containing dyes (quercetin and tannic acid) could facilitate the creation of hydrogen bonds and/or electrostatic interactions with the fiber, resulting in a good fixation of the dye on the fabric [12]. As a result, after dyeing, the flavonoids become insoluble in water during washing, enhancing washing fastness [15].

Table 2 The imparted values of dyed Eri silk fabrics dyed with water, EtOH/water, EtOH.

Solvent	Color Value			Color imparted
	L^*	a^*	b^*	
water	76.99	1.93	26.49	Light yellow
Ethanol/water (25:75)	57.16	-0.45	20.58	Yellowish green
Ethanol/water (50:50)	44.61	-2.75	13.47	Dark green
Ethanol/water (75:25)	40.87	-1.38	17.90	Dark green
Ethanol	49.50	-1.69	17.90	Yellowish dark green

Table 3 Color fastness to washing at 40 °C ISO (105-CO6 A1S: 1994).

Solvent	Color staining
Water	4-5
EtOH/Water (25:75)	4-5
EtOH/Water (50:50)	4-5
EtOH/Water (75:25)	3-4
EtOH	3

A comparison of color fastness rating after washing this work to the relevant literature is disclosed in Table 4. It was noticeable that the fastness rating of the present work gave high color staining of 4-5, suggesting a good quality of dyeing fabric, similar to that of the value reported in the literature. This result induces that the extracted dye from *Oroxylum Indicum (L.) bark* using the co-solvent of EtOH/Water (50:50) for Thai Eri silk dyeing has a promising strategy for the dyeing process.

DOI: 10.60101/jarst.2023.251099

Table 4 Color fastness to washing of dyeing silk in the present work compared with the reported value in the literature.

Dye source	Extraction solvent	Fabric	Color staining	Ref.
eucalyptus leaf	water	silk	4-5	[15]
Eucalyptus wood	water	Nylon	4-5	[11]
Calotropis gigantea leaves	water	silk	4-5	[24]
Oroxylumb Indicum (L.) Kurz	EtOH/Water (50:50)	silk	4-5	This work

CONCLUSION

Effect of different solvents for the dye extraction from *Oroxylumb Indicum* (L.) Kurz on the Eri Thai silk dyeing was intensively investigated. Each solvent used for the extraction gave different relative contents of tannic acid and quercetin. Consequently, it further resulted in different properties of fabric dyed, namely, color characteristics and washing fastness rating. From various solvents studied, the extracted dye efficiency was in the order of EtOH/water (50:50) > MeOH/water (50:50) > MeOH ~ EtOH > water. Among various ratios of EtOH/water, EtOH/water (50:50) was still the most efficient for dye extraction. Moreover, the effects of a dose of *Oroxylumb Indicum* (L.) Kurz, temperature, and time were 8.0g/L, 60 °C, and 60 min, considered the optimum extraction condition due to providing the high relative content of tannic acid and quercetin. The consequence led to good quality of fabric Eri silk dyed such as an excellent fastness rating.

ACKNOWLEDGEMENT

The authors acknowledge the Faculty of Liberal Arts and Science, Roi Et Rajabhat University for the equipment facility. This research did not receive any specific grant from funding agencies in the public, commercial, or not-for-profit sectors.

REFERENCES

1. Graham M. Justifying virtual presence in the thai silk industry: Links between data and discourse. Inf Technol Int Dev. 2010;6:57–70.
2. Patichol P, Wongsurawat W, Johri LM. Upgrade strategies in the Thai silk industry: Balancing value promotion and cultural heritage. J Fash Mark Manag. 2014;18:20–35.
3. Lellis B, Fávaro-Polonio CZ, Pamphile JA, Polonio JC. Effects of textile dyes on health and the environment and bioremediation potential of living organisms. Biotechnol Res Innov. 2019;3;275–90.
4. Kulawong S, Chanlek N, Osakoo N. Facile synthesis of hierarchical structure of NaY zeolite using silica from cogon grass for acid blue 185 removal from water. J Environ Chem Eng. 2020;8:104114.
5. Adedokun O, Sanusi YK, Awodugba AO. Solvent-dependent natural dye extraction and its sensitization effect for dye sensitized solar cells. Optik (Stuttg). 2018;174:497–507.
6. Adeel S, Rehman FU, Rafi S, Zia KM, Zuber M. Environmentally friendly plant-based natural dyes: Extraction Methodology and Applications. In: Ozturk M, Hakeem KR, editor. Plant and Human Health, Volume 2. Eswatini: Springer Nature Switzerland AG; 2019. p. 383–415.
7. Dulo B, De Somer T, Phan K, Roosen M, Githaiga J, Raes K, et al. Evaluating the potential of natural dyes from nutshell wastes: Sustainable coloration and functional finishing of wool fabric. Sustain Mater Technol. 2022;34:e00518.
8. Bukhari M, Shahid-ul-Islam N, Shabbir M, Rather LJ, Shahid M, Singh U, et al. Dyeing studies and fastness properties of brown naphtoquinone colorant extracted from Juglans regia L on natural protein fiber using different metal salt mordants. Text Cloth Sustain. 2017;3:1-9.
9. Yusuf M, Shahid M, Khan MI, Khan SA, Khan MA, Mohammad F. Dyeing studies with henna and madder: A research on effect of tin (II) chloride mordant. J Saudi Chem Soc. 2015;19:64–72.
10. Banerjee AN, Kotnala OP, Maulik SR. Dyeing of Eri silk with natural dyes in presence of natural mordants. Indian J Tradit Knowl. 2018;17:396–9.
11. Rossi T, Silva PMS, De Moura LF, Araújo MC, Brito JO, Freeman HS. Waste from eucalyptus wood steaming as a natural dye source for textile fibers. J Clean Prod. 2017;143:303–10.

DOI: 10.60101/jarst.2023.251099

12. Rehman R, Mahmud S, Habib MA, Islam A. Revolution of Silk Dyeing with FL Based Cotton-Reactive Dyes. Int J Text Sci. 2015;4:42–52.
13. Łabowska MB, Michalak I, Detyna J. Methods of extraction, physicochemical properties of alginates and their applications in biomedical field - A review. Open Chem. 2019;17:738–62.
14. Adedokun O, Sanusi YK, Awodugba AO. Solvent dependent natural dye extraction and its sensitization effect for dye sensitized solar cells. Optik. 2018;174:497–507.
15. Mongkholrattanasit R, Kryštůfek J, Wiener J, Viková M. UV protection properties of silk fabric dyed with eucalyptus leaf extract. J Text Inst. 2011;102:272–9.
16. Faraz R, Gokhale M, Gothalwal R. Callus extracts of Oroxylum indicum (L.) Vent containing baicalein have in vitro antioxidant and antibacterial activities. Biotecnol Veg. 2020;20:51–62.
17. Fu Z, Chen R. Study of complexes of tannic acid with Fe(III) and Fe(II). J Anal Methods Chem. 2019;2019:1-6.
18. Srinivas K, King JW, Howard LR, Monrad JK. Solubility and solution thermodynamic properties of quercetin and quercetin dihydrate in subcritical water. J Food Eng. 2010;100:208–18.
19. Ranoszek-Soliwoda K, Tomaszewska E, Socha E, Krzyczmonik P, Ignaczak A, Orlowski P, et al. The role of tannic acid and sodium citrate in the synthesis of silver nanoparticles. J Nanoparticle Res. 2017;19:1–15.
20. Porto ICCM, Nascimento TG, Oliveira JMS, Freitas PH, Haimeur A, França R. Use of polyphenols as a strategy to prevent bond degradation in the dentin–resin interface. Eur J Oral Sci. 2018;126: 146–58.
21. Jagetia GC. A Review on the Medicinal and Pharmacological Properties. Sinusitis. 2021;5:71–89.
22. Wettasinghe M, Shahidi F. Antioxidant and free radical-scavenging properties of ethanolic extracts of defatted borage (Borago officinalis L.) seeds. Food Chem. 1999;67:399–414.
23. Soares AT, Júnior JGM, Lopes RG, Derner RB, Filho NRA. Improvement of the extraction process for high commercial value pigments from desmodesmus sp. Microalgae. J Braz Chem Soc. 2016;27:1083–93.
24. Nugraha J, Sukmawati A, Mulyawan AS, Sugiyana D. Biduri (Calotropis gigantea) leaves extract as natural dyes and ultraviolet protector applied on silk fabric with an exhaust dyeing method. IOP Conf Ser Mater Sci Eng. 2020;980:012021.

DOI: 10.60101/jarst.2023.251099

Received: January 1, 2023 | Revised: April 19, 2023 | Accepted: April 19, 2023

JOURNAL OF APPLIED RESEARCH ON SCIENCE AND TECHNOLOGY
JARST
INSTITUTE OF RESEARCH AND DEVELOPMENT
RAJAMANGALA UNIVERSITY OF TECHNOLOGY THANYABURI
ISSN ONLINE: 2773-9473
https://ph01.tci-thaijo.org/index.php/
rmutt-journal

Smart meter design for energy consumption monitoring of residential premises

Muhammad Mansattha[1], Hassan Dao[2*] and Arfip Jikaraji[2]

[1]Department of Electrical Engineering, Faculty of Engineering, Princess of Naradhiwas University, Narathiwat 96000, THAILAND

[2]Department of Computer Engineering, Faculty of Engineering, Princess of Naradhiwas University, Narathiwat 96000, THAILAND

[*]Corresponding author e-mail: hassan@pnu.ac.th

ABSTRACT

Electricity consumption is a crucial issue for economic development, especially in the residential sector. The number of households has increased significantly despite the declining availability of energy resources. There is a clear need for an efficient electricity consumption monitoring system that can provide accurate data on residential energy consumption. This paper proposes an Internet of Things (IoT)-based smart meter system design for monitoring household energy consumption. The system employs hardware and IoT technology, specifically the Node-MCU of ESP-32 and an ADE7757 power sensor module which runs on a 5(15) Amp of a single-phase meter. The energy consumption data is logged in cloud storage using the AppSheet platform hosted on Google Cloud. The system features digital displays and consumption analytics, allowing consumers to collect and transmit data about their energy usage. Energy usage data provides consumers accurate and timely information about their energy consumption. This information can help them better manage and reduce their energy usage. The system also offers the estimation of the energy consumption for individual appliances with a user-friendly monitoring experience for the energy sector. The proposed smart meter system has been evaluated using 1,080 data sets, with an average accuracy rate of 1.48% compared to a 5(15) Amp, single-phase meter. Additionally, the system can predict energy charges with an accuracy of 0.02% based on the schedule of residential electricity tariff regulated by the Provincial Electricity Agency (PEA), Thailand. These results show that the system is highly accurate and can promote positive user behavior towards better energy supply and demand management, reduced energy waste, and improved system reliability. The features of smart meter systems enable consumers and utilities to make more informed decisions about energy usage, promoting more efficient and sustainable energy practices.

Keywords: IoT, Smart Meter, Energy Consumption, Residential Premises

INTRODUCTION

Inconsistency between demand and supply of electric energy is challenged in the context of sustainability. Energy shortage and rapid growing of electric energy consumption has become broadly studied throughout the world in terms of economic development [1-4].

Energy efficiency is prime concerned in two main aspects upon which issues can arise. On one hand, environmental awareness relates to management and prevention of consequences caused by energy wastage. On the other hand, economic aspect concerns cost reduction to achieve counterbalance [3, 5-7]. Since the energy cost tends to increase gradually, new technologies have been invented to reduce electric consumption. In this situation, energy efficiency of most types of appliances, electrical and control devices is continually sought to be improved in industrial, residential and business sector [8–10]. Many consumers intent to reduce their energy consumption.

According to International Energy Agency, 68% of energy consumption and greenhouse gas emission are mainly attributed to residential and commercial buildings. Reduction of energy consumption and emission in such sectors are crucial for long-term transition (11, 12). Energy consumption statistics in Thailand between 2002 and 2018 recorded by Energy Policy and Planning office (EPPO), Ministry of Energy, Thailand found that residential sector is responsible for the second highest consumption as shown in Figure 1.

Zhao et al. [1] developed an energy monitoring system for large public buildings. The system utilizes sensors to collect energy consumption data and displays the data on a user-friendly interface. The authors also

DOI: 10.60101/jarst.2023.250745

highlight the importance of technical details, potential benefits of the system, sustainable practices, and energy efficiency in public buildings, emphasizing that the energy monitoring system can help achieve these goals by reducing energy costs and promoting more sustainable practices.

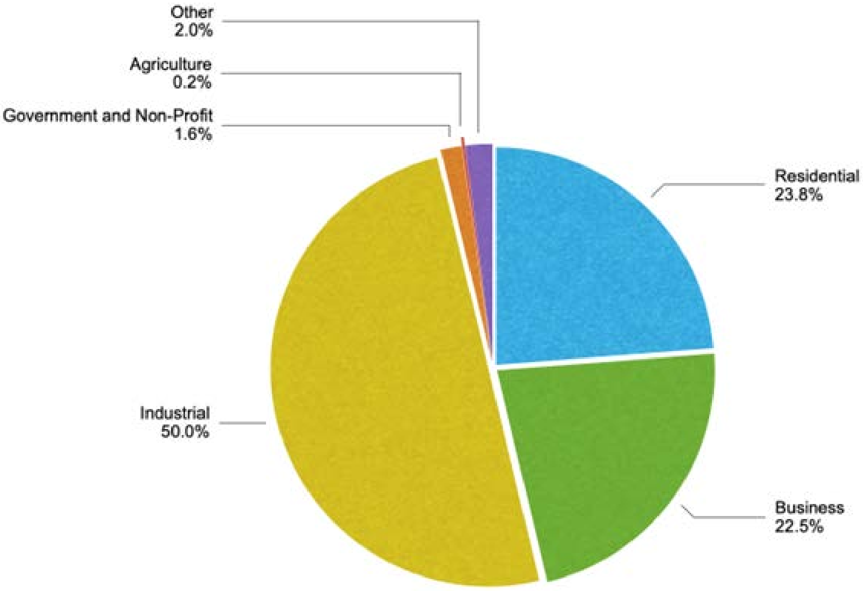

Figure 1 Electric consumption by sectors in Thailand between 2002 and 2018.

Marques and Pitarma [5] presented a wireless energy monitoring system designed to collect and display real-time energy consumption data in households and buildings. The authors describe the technical aspects of the system, including its hardware and software components, data processing methods, and visualization techniques. The article also emphasizes the potential benefits of the system, such as identifying areas of energy waste and promoting energy conservation. The authors conclude that the system has the potential to significantly reduce energy costs and promote sustainable practices in households and buildings.

Luan and Leng [10] presented a monitoring system that utilizes the Internet of Things (IoT) for smart energy management in a building. The system consists of wireless sensor nodes that monitor various parameters related to energy consumption, such as temperature, humidity, and light intensity. The data is collected and transmitted wirelessly to a central server, where it is analysed and used to optimize energy consumption. The authors provide a detailed description of the hardware and software components of the system and report on the system's performance in a real-world deployment. The study demonstrates the potential of IoT-based systems for effective energy management in buildings, with the ability to optimize energy consumption and reduce costs.

Sučić et al. [11] presented a study on the design and implementation of an energy monitoring system for residential buildings. The system is designed to monitor energy consumption in real-time and provide feedback to the occupants to encourage more efficient energy usage. The authors describe the hardware and software components of the system, which include a smart meter, sensors, and a user interface. The system is tested in a residential building, and the results indicate that it is effective in monitoring and analysing energy consumption patterns. The system provides feedback to users through a user interface, which can be accessed via mobile devices or computers. The authors conclude that the system has the potential to significantly reduce energy consumption in residential buildings and contribute to the overall goal of sustainability.

Several studies have shown that energy consumption in buildings can be influenced by user behaviour, despite overall consumption being considered a dominant characteristic. However, traditional methods of measurement have been shown to be inefficient in changing consumer behavior [11, 13-15]. Therefore, an energy monitoring tool is essential to help manage energy and avoid wastage, allowing for more efficient decision-making and changes to consumption routines [16, 17].

The Provincial Electricity Agency (PEA), Thailand categorises electricity tariffs [18] into 8 schedules namely, residential, small general service, medium general service, large general service, specific business service, non-profit organization, agricultural pumping, and temporary service.

This paper presents the design of an electricity consumption monitoring system using a single-phase meter with a 5(15) Amp rating and energy charge prediction based on Thailand's PEA residential

DOI: 10.60101/jarst.2023.250745

electrical tariff schedule. The system, which includes wireless communication for remote monitoring, is compared to a standard PEA meter and provides users with an easy way to monitor their electricity consumption and performance.

MATERIALS AND METHODS

The proposed energy monitoring system design comprises three primary components: Cloud of Things (CoT), Smart meter nodes, and Software design, as illustrated in Figure 2. The smart meter node serves as a mediator between an AC power source and an electrical appliance. It is equipped with voltage and current sensors (ADE7757) that accurately measure energy consumption.

The embedded Node-MCU within the smart meter then transmits this information to the cloud platform every ten minutes, allowing easy access and data analysis from each meter node. The data obtained from the smart meter nodes enables users to identify areas of high energy consumption and compare energy usage across different nodes.

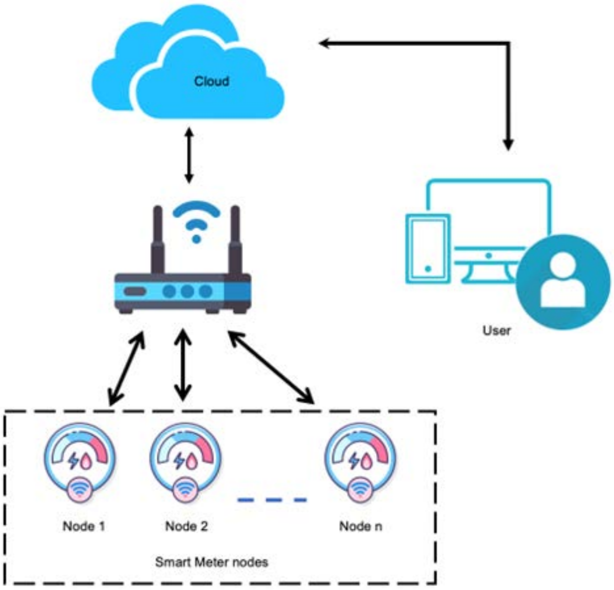

Figure 2 Designed overview of proposed electricity consumption monitoring system.

Cloud of Things (CoT)

CoT is a combination of Cloud and Internet of Things (IoT), which enables the transfer of computer functionalities from local computers to the cloud [19]. This technology can be applied in various optimal solutions where users no longer need to worry about resource maintenance, local storage, or application installation. AppSheet platform is an example of a cloud-based platform that supports both mobile operating systems and web platforms. AppSheet apps provide on-premise data integration with several data sources [20, 21].

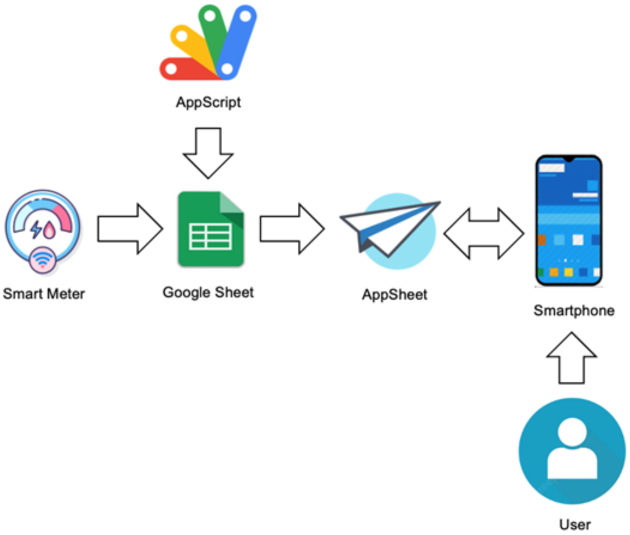

Figure 3 Data-driven application for Smart meter monitoring system.

Data-driven applications are essential for effective communication and data exchange. Figure 3 illustrates the framework of the energy monitoring system. Smart meter nodes initially acquire the energy consumption data, which are then updated and transferred to a spreadsheet using Appscript. The collected data are visualised in application using Appsheet.

Smart meter node

Smart meter nodes are strategically placed based on the monitoring requirements and comprise two main components: the Node-MCU of ESP32 and the ADE7757 Power sensor. The smart meter nodes are installed between the AC source and the electrical appliance or socket requiring monitoring. ESP32 features an open-source microcontroller and a WiFi microchip. The ADE7757 sensor is considered a precise electrical energy measurement tool. After receiving the voltage and current outputs from the load through the power sensor, the data is transmitted to the ESP32, which calculates the energy consumption parameters and energy charges, displaying them on an LCD and transmitting the data via WiFi to the server. The smart meter node diagram in Figure 4 depicts this process.

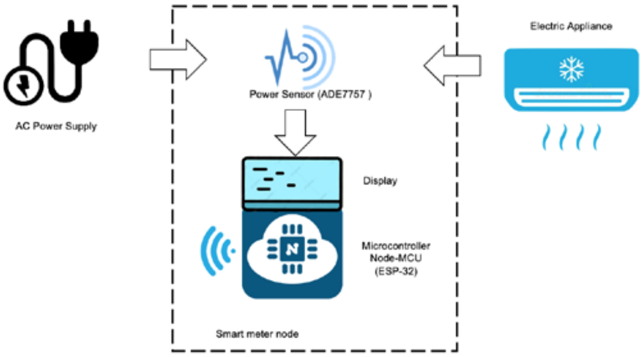

Figure 4 Design of proposed smart meter node.

DOI: 10.60101/jarst.2023.250745

Figure 5 shows the signal process diagram of ADE7757 [22, 23], which outlines the process of digitizing the voltage signal input using voltage and current sensors. Initially, the DC component of the instantaneous power signals is removed using a high-pass filter as the IC is intended to operate with AC input. Subsequently, the instantaneous power signal is multiplied directly by the current and voltage signals, which yields the instantaneous real power component from the previous signal of the low-pass filter.

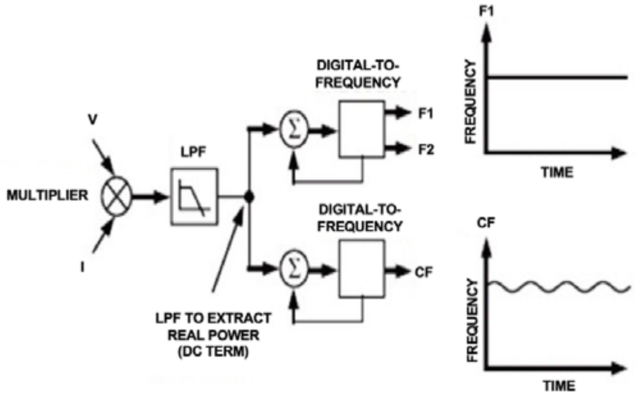

Figure 5 Real Power-to-Frequency Conversion process.

The digital-to-frequency converter generates an output frequency based on the real power component. This output frequency is then processed in the digital domain and connected to a counter in the microcontroller. The counter calculates the number of pulses for a specific interval, enabling the expression of the average power as a proportion to the average frequency using equation (1) [22-24]:

$$F_{avg} = P_{avg} = \frac{Counter}{Time} \quad (1)$$

where F_{avg} is Average frequency and P_{avg} is Average power.

The relationship between energy and counter is defined by (2).

$$Energy = P_{avg} \times Time$$

$$= \frac{Counter}{Time} \times Time = Counter \quad (2)$$

The calibration process is crucial to guarantee the precise accumulation of pulses and eliminate any ripple frequency. To perform calibration, the pulse frequency is manually measured using an oscilloscope, ranging from 0.4 to 5.08 V. Under steady load conditions and at a voltage of 220 V, ten different current levels are measured, resulting in 1,080 data set. The corresponding number of pulses per minute (PPM) is then recorded and summarized in Table 1.

The relationship between the number of PPM and current is described by equation (3). The linear relationship between the number of PPM and the current levels is determined by fitting a straight line to the measured PPM values for current levels ranging between 0.4 - 5.08 A at 220 V as shown in Figure 6.

$$F = 13.685I + 2.084 \quad (3)$$

Table 1 Number of PPM at steady currents and voltages.

Current (A)	Voltage (V)						
	200	205	210	215	220	225	230
1.43	19.2	19.7	20.2	20.6	21.1	21.6	22.1
2.08	26.2	26.9	27.5	28.2	28.8	29.5	30.2
2.45	32.5	33.3	34.1	34.9	35.7	36.5	37.3
3.02	39.0	39.9	40.9	41.9	42.9	43.8	44.8
3.5	45.5	46.6	47.7	48.9	50.0	51.1	52.3
4.05	52.4	53.8	55.1	56.4	57.7	59.0	60.3
4.53	59.3	60.8	62.2	63.7	65.2	66.7	68.2
5.08	65.1	66.7	68.3	70.0	71.6	73.2	74.9

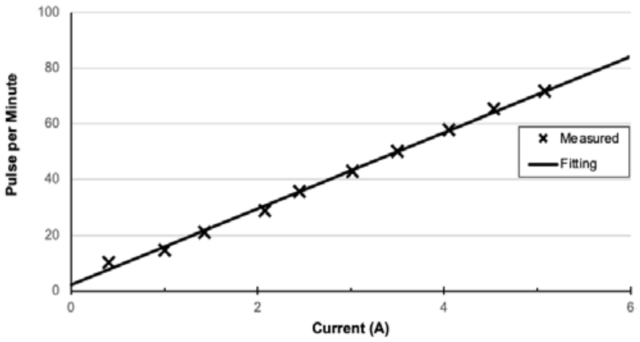

Figure 6 Relationship between number of PPM for given currents at 220 V.

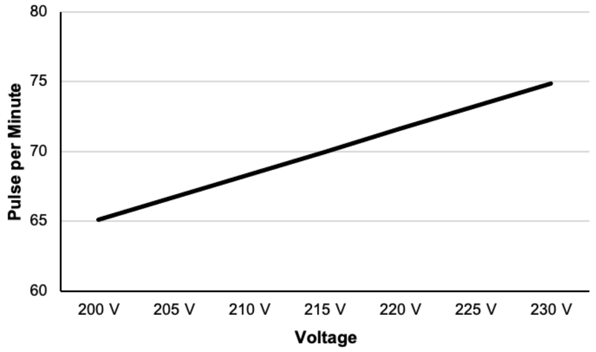

Figure 7 Measurement of number of PPM at 5.08 A for given voltages.

DOI: 10.60101/jarst.2023.250745

Figure 7 demonstrates a linear increase in the number of PPM with the voltage, ranging from 200-230 V at a current of 5.08 A. Specifically, the number of PPM increases linearly between 65 and 75 PPM.

Software Design

The flowchart diagram used in the design of smart meter node is shown in Figure 8.

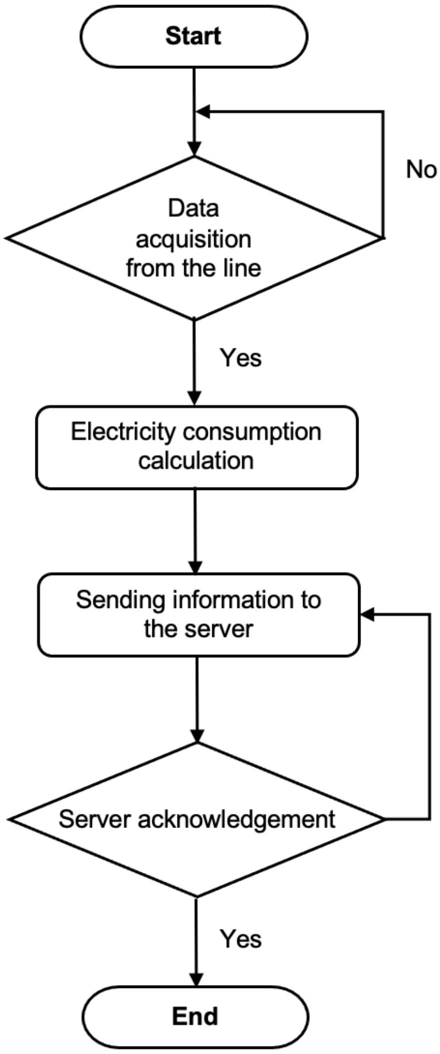

Figure 8 Process diagram of a smart meter node.

Initially, the power signal is acquired from the line using the power sensor, followed by the calculation of electricity consumption by the microcontroller. The energy charge is then determined based on the residential electricity tariff schedule in Table 2, measured in baht per kilowatt-hour (kWh). Additionally, a service charge of 8.19 baht per month is applied [25].

Table 2 Schedule of residential electricity tariff.

Unit charge(kWh)	Energy Charge(baht/kWh)
0-15th	2.3488
16th-25th	2.9883
26th – 35th	3.2405
36th – 100th	3.6237
101st – 150th	4.2218
151st – 400th	4.4217

Once the smart meter node calculates electricity consumption and determines the energy charge. it transmits this information to the server and awaits confirmation. In case no acknowledgement is received from the server, the microcontroller is programmed to re-send the information after every ten-minute interval until a response is received.

Calculating the percentage difference between a measurement and from a meter is crucial to compare and assess the accuracy of the smart measure node and the PEA meter. The percentage difference can determine by equation (4) [26].

$$|(PEM - SMN)/SMN| \times 100\% \qquad (4)$$

Where PEM is PEA meter and SMN is the smart meter node.

RESULTS AND DISCUSSION

The energy consumption is measured and compared between the standard PEA meter and the smart meter node at 220 V. The energy charge is also computed for given steady currents based on residential tariff, using Table 2. In addition, the results are recorded in Table 3, which compares the electricity unit consumption and energy charge between the standard consumer meter (PEM) and smart meter node (SMN). The findings show that the smart meter has an average accuracy of 1.48% in measuring energy consumption and can predict energy charges with a high precision, with only a 0.02% deviation.

Table3 Comparison of standard consumer meter of PEA and smart meter node for given currents and interval times.

Current (A)	Time (Minute)	Electricity Unit		Electricity Charge (Baht)	
		SMN	PEM	SMN	PEM
3.5	4	0.05	0.06	8.31	8.32
	6	0.08	0.08	8.38	8.38
	8	0.11	0.11	8.45	8.45
	10	0.14	0.14	8.52	8.52

DOI: 10.60101/jarst.2023.250745

Current (A)	Time (Minute)	Electricity Unit		Electricity Charge (Baht)	
		SMN	PEM	SMN	PEM
4.0	4	0.06	0.06	8.33	8.33
	6	0.1	0.10	8.42	8.42
	8	0.13	0.13	8.50	8.50
	10	0.17	0.16	8.59	8.57
4.5	4	0.06	0.07	8.35	8.35
	6	0.11	0.11	8.45	8.45
	8	0.14	0.14	8.52	8.52
	10	0.18	0.18	8.61	8.61
5.0	4	0.08	0.08	8.38	8.38
	6	0.12	0.12	8.47	8.47
	8	0.17	0.16	8.59	8.56
	10	0.21	0.20	8.68	8.66

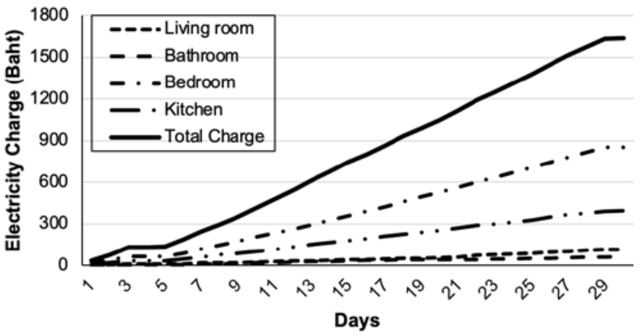

Figure 9 Electricity charge of different nodes for 30 days.

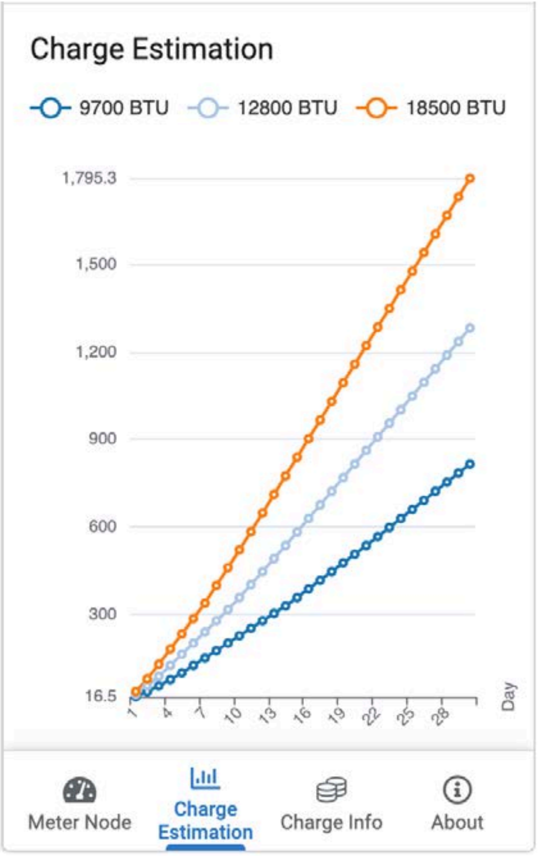

Figure 10 Estimation of electricity charges for air conditioners with varying BTU provided by the smart meter application.

The monitoring system performance is tested using variety of appliance installed in different home partitions. The smart meter has potential to measure energy consumption which depends on the load on devices. The series of collected data are converted to electricity charge and then visualize in the application. Figure 9 exemplifies the electricity charge of five different rooms in a house, namely the kitchen, bedroom, bathroom, living room and total charge for thirty days.

Furthermore, the smart meter has the capability to estimate the electricity charges for individual appliances by considering their power consumption and daily usage time. Figure 10 demonstrates this feature by showing the electricity charge for an air conditioner over a period of 30 days, calculated based on three different British Thermal Units (BTU). This valuable tool allows users to make informed decisions about which appliances to purchase, as they can estimate the potential electricity costs associated with their usage beforehand. Overall, the smart meter provides a convenient and helpful solution for monitoring and managing electricity usage, empowering users to make more informed decisions about their energy consumption.

CONCLUSION

The design of energy consumption monitoring system is presented in this paper based on residential tariff. CoT is capable to communicate and update the smart meter nodes in real-time. Thus, the users unnecessary require local storage and resource maintenance.

The energy consumption and energy charge are presented and compared between standard PEA meter and smart meter node at 220 V for given currents. The results show that the smart meter can measure the energy consumption and charge accurately compared to the standard meter. The findings show that the smart meter has an average accuracy of 1.48% in measuring energy consumption and can predict energy charges with high precision, with only a 0.02% deviation.

DOI: 10.60101/jarst.2023.250745

The proposed smart meter system is a well-designed integration of cloud-based technology and IoT for efficient energy consumption monitoring and accurate charge prediction. The system features digital displays and consumption analytics, allowing consumers to collect and transmit data about their energy usage. The energy usage data is used to provide consumers with accurate and timely information about their energy consumption. Additionally, the system also offers the estimation of the energy consumption for individual appliances with a user-friendly monitoring experience for the energy sector.

It is recommended to extend the electricity charge computation for 15(45) Amp meter or larger, as there are different schedules of electricity tariff for such meters. Overall, this system can be beneficial for both residential and commercial applications, as it enables remote monitoring and comparison of energy consumption across multiple nodes. The implementation of this system can not only improve energy efficiency but also increase awareness and promote more sustainable energy practices. Thus, identifying opportunities for potential energy savings.

REFERRENCES

1. Zhao L, Zhang JL, Liang RB. Development of an energy monitoring system for large public buildings. Energy Build. 2013;66:41-8.
2. Nader W. Real-time power monitoring, home automation and sustainability [dissertation]. Faculty of the graduate college: University of Nebraska - Lincoln; 2011.
3. York R, McGee JA. Does renewable energy development decouple economic growth from CO_2 emissions?. Socius Sociol Res a Dyn World. 2017;3:1-6.
4. Dai H, Xie X, Xie Y, Liu J, Masui T. Green growth: The economic impacts of large-scale renewable energy development in China. Appl Energ. 2016;162:435–49.
5. Marques G, Pitarma R. Monitoring energy consumption system to improve energy efficiency. In: Rocha A, Correia AM, Adeli H, Reis LP, Costanzo S, editors. Recent Advances in Information Systems and Technologies. WorldCIST 2017: Proceedings of the 2017 World Conference on Information Systems and Technologies (WorldCIST'17); 2017 Apr 11-13; Madeira, Portugal. Berlin: Springer; 2017.
6. Almasri RA, Almarshoud AF, Omar HM, Esmaeil KK, Alshitawi M. Exergy and economic analysis of energy consumption in the residential sector of the qassim region in the Kingdom of Saudi Arabia. Sustainability.2020;12(7):2606.
7. Stern DI. The Role of Energy in Economic Growth. SSRN Electronic Journal [Internet]. 2012 [cited 2022 Nov. 24]. Available from: https://papers.ssrn.com/sol3/papers.cfm?abstract_id=1715855
8. Rojas-Renteria JL, Espinoza-Huerta TD, Tovar-Pacheco FS, Gonzalez-Perez JL, Lozano-Dorantes R. An electrical energy consumption monitoring and forecasting system. Engineering, Technology & Applied Science Research. 2016; 6(5):1130–2.
9. Mir AA, Alghassab M, Ullah K, Khan ZA, Lu Y, Imran M. A review of electricity demand forecasting in low and middle income countries: The demand determinants and horizons. Sustainability. 2020;12:5931.
10. Luan H, Leng J. Design of energy monitoring system based on IOT. Proceedings of the 2016 Chinese Control and Decision Conference (CCDC); 2016 May 28-30; Yinchuan, China. New York: IEEE; 2016.
11. Sučić B, Anđelković AS, Tomšić Ž. The concept of an integrated performance monitoring system for promotion of energy awareness in buildings. Energy Build. 2015;98:82–91.
12. Wang Q, Kwan MP, Zhou K, Fan J, Wang Y, Zhan D. Impacts of residential energy consumption on the health burden of household air pollution: Evidence from 135 countries. Energ Policy. 2019;128:284–95.
13. Viciana E, Alcayde A, Montoya FG, Baños R, Arrabal-Campos FM, Zapata-Sierra A, et al. OpenZmeter: An efficient low-cost energy smart meter and power quality analyzer. Sustainability. 2018;10:4038.
14. Guerra Santin O, Itard L, Visscher H. The effect of occupancy and building characteristics on energy use for space and water heating in Dutch residential stock. Energy Build. 2009; 41(11):1223-32.
15. De Meester T, Marique AF, De Herde A, Reiter S. Impacts of occupant behaviours on residential heating consumption for detached houses in a temperate climate in the northern part of Europe. Energy Build. 2013;57:313-23.
16. Subhash R, Balaji VR, Sanjana KE, Madhavan N, Siva T. Smart Automated Energy Meter. In: Shilpi G, Jignesh N, editors. ET2ECN 2020: Third International Conference, ET2ECN 2020; 2020 Feb 7-8; Surat, India. Berlin: Springer; 2020. p. 19–28.
17. Alahakoon D, Yu X. Smart electricity meter data intelligence for future energy systems: A survey. IEEE Transactions on Industrial Informatics. 2016;21(1):425-36.

DOI: 10.60101/jarst.2023.250745

18. Ministry of Energy. Electricity [Internet]. Bangkok: Energy Policy and Planning office (EPPO) Ministry of Energy; [cited 2021 Oct 22]. Available from: https://www.eppo.go.th/index.php/en/en-energystatistics/electricity-statistic
19. Xuan S, Kim DH. Development of cloud of things based on proxy using OCF IoTivity and MQTT for P2P internetworking. Peer-to-Peer Networking and Applications. 2020;13(3):729-41.
20. Petrovic N, Roblek V, Radenković M, Nejkovic V. Approach to Rapid Development of Data-Driven Applications for Smart Cities using AppSheet and Apps Script. 10th International Conference on Applied Information and Internet Technologies - AIIT 2020. Berlin: Researchgate; 2020.
21. Petrovic N, Radenković M, Nejkovic V. Data-Driven Mobile Applications Based on AppSheet as Support in COVID-19 Crisis. IcETRAN 2020: Berlin: Researchgate; 2020.
22. Ghodki MK. Microcontroller and solar power based electrical energy management system for renewable energy applications. International Journal of Electrical Power & Energy Systems. 2013;44(1):852-60.
23. Stephen T. English. A Low Cost Watt-Hour Energy Meter Based on the ADE7757 [Internet]. Diepoldsau: YUMPU [cited 2023 May 2]. Available from: https://www.yumpu.com/en/document/view/17949903/a-low-cost-watt-hour-energy-meter-based-on-the-ade7757-
24. Bharath P, Ananth N, Vijetha S, Jyothi PKV. Wireless automated digital energy meter. 2008 IEEE International Conference on Sustainable Energy Technologies. 2008 Nov 24-27; Singapore: IEEE; 2009.
25. (PEA) TPEA. Electricity Tariff 2018 [Internet]. Bangkok: Provincial Electricity Authority [cited 2021 Oct 22]. Available from: https://www.pea.co.th/en/ electricity-tariffs/
26. Bevington P, Robinson DK. Data Reduction and Error Analysis for the Physical Sciences. USA: McGraw-Hill Education; 2002.

DOI: 10.60101/jarst.2023.250745

Received: April 25, 2023 | Revised: July 25, 2023 | Accepted: July 31, 2023

JARST
JOURNAL OF APPLIED RESEARCH ON SCIENCE AND TECHNOLOGY
INSTITUTE OF RESEARCH AND DEVELOPMENT
RAJAMANGALA UNIVERSITY OF TECHNOLOGY THANYABURI
ISSN ONLINE: 2773-9473
https://ph01.tci-thaijo.org/index.php/rmutt-journal

Mixed Bootstrap-Marascuilo test for testing equality of means under unequal variances in a completely randomized design

Phannipa Worapun[1] and Tammarat Kleebmek[2*]

[1]Department of Applied Mathematics and Statistics, Faculty of Sciences and Liberal Arts, Rajamangala University of Technology Isan, Nakhon Ratchasima 30000, THAILAND

[2]Department of Statistics, Faculty of Science, Khon Kaen University, Khon Kaen 40002, THAILAND

[*]Corresponding author e-mail: tammarat@kku.ac.th

ABSTRACT

This study introduces a pioneering statistical methodology, the Mixed Bootstrap-Marascuilo test, which emerges from the fusion of the Bootstrap method and the Marascuilo test. The test examines the means of three or more populations with unequal variances in a completely randomized design. The research compares the Mixed Bootstrap-Marascuilo test's ability to control the probability of type I error using Cochran's criteria and its test power using penalized power with those of One-Way ANOVA and the Marascuilo test. The research design thoughtfully encompasses three populations: small, medium, and large, each exhibiting variations in size and equality. It systematically manipulates variances, encompassing a range from equal to slightly different, moderately different, and significantly different. Furthermore, the error distribution is specified to be normal with a designated mean. The research methodology embraces the utilization of R ver.4.2.2 and the Monte Carlo technique, leveraging 5,000 simulations per case to ensure the robustness and reliability of the study's findings. The outcomes of the comprehensive analysis yield intriguing insights. The results indicate that the Mixed Bootstrap-Marascuilo test exhibits superior testing ability in scenarios involving equal small sample sizes with equal and moderate variances, as well as medium sample sizes with equal and small variances. Furthermore, it demonstrates effectiveness even when dealing with large, unequal sample sizes with equal and large variances. In essence, this research advances the realm of statistical hypothesis testing through the introduction and meticulous evaluation of the Mixed Bootstrap-Marascuilo test. Its demonstrated ability to navigate complexities in mean examination across diverse populations, coupled with its versatile applicability to scenarios of unequal variances and varying sample sizes, underscores its potential as a valuable tool for researchers across disciplines.

Keywords: Unequal variances, ANOVA, Bootstrap, Marascuilo test, Mixed Bootstrap-Marascuilo test

INTRODUCTION

Statistical analysis is essential to most research studies and is crucial to data analysis. In experimental research, where experimental design is a critical step, statistical methods are necessary to ensure reliable results. Researchers need to have statistical knowledge to analyze data and select appropriate statistical methods based on the characteristics of the data, in addition to subject matter expertise and the ability to design experiments. The Completely Randomized Design (CRD) is a data analysis technique used for a single factor with several levels, requiring the experimental units to be similar. The One-Way Analysis of Variance (One-Way ANOVA) is the analysis method employed. However, in practice, the data may not adhere to the initial assumption that the error follows a normal distribution and homogeneity of variance, particularly when the variances of each population are different. Using the ANOVA technique under such conditions may result in inaccurate conclusions. To address this, statisticians have developed and refined tests to evaluate the difference in means among multiple population groups when analyzing data with unequal variances. Examples of such tests include Welch's Test, Marascuilo Test, Brown-Forsythe's Test, Modified Brown-Forsythe's Test, Generalized F Test, and others. Komduan [1] conducted a comparative study of the Welch test, Brown-Forsythe test, Marascuilo test, and Parametric

DOI: 10.60101/jarst.2023.251663

Bootstrap approach. The study revealed that the Welch test and Marascuilo test effectively controlled the probability of Type I error and had the highest testing power when the error followed a normal distribution and the variance of the error differed. Hananurak [2] also found that the Marascuilo test could control Type I error probability when the population followed a t-distribution and had the highest testing capacity when the population was normally distributed. Additionally, Efron and Tibshirani [3] and Sangthong [4] proposed a parameter estimation method that includes estimating the variance of various estimators, known as the Bootstrap technique. Reiczigel et al. [5] compared the Bootstrap Rank-Welch (BRW) test with the Wilcoxon-Mann-Whitney (WMW) test, the Rank Welch (RW) test, and the Brunner-Mansel (BM) test. They found that the BM test could control the probability of error well in a large sample, and the Bootstrap Rank-Welch test could control the probability of error as well as the Wilcoxon-Man-Whitney test and the Rank-Welch test in a small sample. Dag et.al. [6] compared seven one-way tests in the oneway tests package. The Kruskal-Wallis test performs best with small and medium effect sizes. Cavus and Yazaci [7] present the doex package, which contains the tests for equality of normal distributed and independent group means under unequal variances. Although new test statistics are continually being proposed, it remains unclear which test statistics are most effective under the same circumstances. Thus, this study aims to compare the statistical efficiency of three tests: One-Way ANOVA, Marascuilo procedure, and a novel approach that combines the Marascuilo test procedure with the Bootstrap technique called the Mixed Bootstrap-Marascuilo (MBM) test. The study examines scenarios involving normal distributions, varying variances, and equal or unequal sample sizes across three populations. The primary criterion for assessing performance is controlling Type I error rates and achieving the highest testing power.

MATERIALS AND METHODS

The Completely Randomized Design (CRD) is a trial scheme randomly assigning treatments to trial units without specific conditions or restrictions. This design ensures that each trial unit has an equal chance of receiving any treatments, making it most like the trial units themselves. The primary goal of CRD is to compare the means of k populations.

$$y_{ij}=\mu+\tau_i+\varepsilon_{ij} \qquad (1)$$

$i = 1,2,\ldots\ldots,k, j = 1,2,\ldots\ldots,n_i$

where

n_i is the number of the ith treatment,

y_{ij} is the jth observation of the ith treatment,

μ is the population mean,

τ_i is the treatment effect of the ith treatment,

and ε_{ij} is the random error.

The null hypothesis is simply that all the group population means are the same. The alternative hypothesis is that at least one pair of means is different. For example, if there are k groups:

$$H_0: \mu_1 = \mu_2 = \mu_3 = \cdots = \mu_k$$

H_1: At least one of the group's means is different.

1. The method of test statistics

This study is experimental research that aims to compare the efficiency of test statistics for comparing population means across three or more groups, specifically the One-Way ANOVA, Marascuilo Test, and the Mixed Bootstrap-Marascuilo Test obtained by applying the bootstrap technique to the Marascuilo test statistics. The RStudio program was used to simulate data and test hypotheses. The research methodology is described as follows:

1.1 One-Way ANOVA

The One-Way ANOVA is applied to assess whether there are statistically significant distinctions among the means of three or more independent (unrelated) groups. There are two primary assumptions: the responses for each factor level have a normal population distribution. These distributions have the same variance. Examining the formula for One-Way ANOVA as shown in Table 1.

Table 1 One-way ANOVA Table.

SV	***DF***	***SS***	***MS***	$\boldsymbol{F_{cal}}$
Treatment	$k-1$	$SSTr$	$MSTr$	$\frac{MSTr}{MSE}$
Error	$\sum n_i - k$	SSE	MSE	
Total	$\sum n_i - 1$	SST		

where SV : Source of Variation,

DF : Degree of Freedom,

SS : Sum of Square,

MS : Mean Square.

We have

$$F_{cal} = \frac{MSTr}{MSE}$$

where $MSE = \frac{SSE}{\sum n_i - k}$, $MSTr = \frac{SSTr}{k-1}$,

$SSTr$: treatment sum of square

$$SSTr = \sum_{i=1}^{k} \frac{y_{i.}^2}{n_i} - \frac{y_{..}^2}{\sum n_i - k},$$

SSE : Error sum of square

$$SSE = \sum_{i=1}^{k}\sum_{j=1}^{n} y_{ij}^2 - \sum_{i=1}^{k} \frac{y_{i.}^2}{n_i}$$

and

$$SSE = SST - SSTr,$$

to reject H_0 when $F_{cal} > F_{\alpha,k-1,\sum n_i - k}$.

1.2 Marascuilo test

Marascuilo (M) test [8] is a modified version of the Welch test, simplifying the calculation process. It is a method for testing the equality of means in more than two populations in cases where the variances are unequal. This test is suitable for large sample sizes and for groups with different population variances. Let's delve into the formula for the Marascuilo test:

$$M = \sum_{i=1}^{k} w_i[\bar{y}_i - \tilde{y})^2/(k-1)]$$

where $w_i = \frac{n_i}{s_i^2}, u = \sum_{i=1}^{k} w_i , \tilde{x} = \sum_{i=1}^{k} \frac{w_i \bar{y}_i}{u}$.

$\bar{y}_i$ is mean of the i^th^ treatment,
s_i^2 is variance of the i^th^ treatment
To reject H_0 when $M > F_{\alpha,k-1,f}$

$$f = \left[\frac{3}{(k^2-1)}\left(\sum_{i=1}^{k} \frac{\left(1-\frac{w_i}{u}\right)^2}{n_i - 1}\right)\right]^{-1}$$

At the level of significant α

1.3 The Mixed Bootstrap-Marascuilo test (MBM)

The test is obtained by applying the bootstrap technique to the Marascuilo test statistics, which are described as follows:

1.3.1 Let $Y_i = y_{i1}, y_{i2}, \ldots, y_{in_i}$ is an observation from sample i, sample size n_i and have a normal distribution.

1.3.2 A random sampling with replacement by using the technics Bootstrap, Define $Y_i^* = y_{i1}^*, y_{i2}^*, \ldots, y_{in_i}^*$ from n_i^* which is sample size equal n_i.

1.3.3 To compute the test of Marascuilo (M^*) from the sample Y_i^*, n_i^* as follows:

$$M^* = \sum_{i=1}^{k} w_i^*[(\bar{y}_i^* - \tilde{y}^*)^2/(k^*-1)]$$

where

$$w_i^* = \frac{n_i^*}{s_i^{2*}}, u^* = \sum_{i=1}^{k} w_i^* , \tilde{y}^* = \sum_{i=1}^{k} \frac{w_i^* \bar{y}_i^*}{u^*} .$$

1.3.4 Repeat step 3 until 5,000 rounds have been completed.

1.3.5 Take the test statistics obtained from the 5,000 rounds of bootstrap sampling to find the mean, and compare the mean of the test statistics obtained with the critical.

2. The simulation and compare the test statistics

The study was conducted using the Monte Carlo data simulation method. The R programming language (version 4.2.2) was used to simulate data and test hypotheses. The operating procedures were designed to determine α_i is the probability of a type I error of the test (to reject the null hypothesis when it is true), in comparison to the Bradley criteria [9], and used penalized power introduced by Cavus et.al. [10] to compare the power of the test as follows:

$$\gamma = \frac{1-\beta}{\sqrt{1+\left|1-\frac{\alpha_i}{\alpha_0}\right|}}$$

where β is type II error and α_0 is the nominal level. The procedures are as follows:

1) Set the criteria for determining the effectiveness of controlling the probability of Type I errors from Bradley [9]. If the probability of a Type I error resulting from the experiment falls within the range specified for each level of significance, it means that the test statistic can control the Type I error probability. It can be classified according to the significance level, as shown in Table 2.

Table 2 The level of significant of Type 1 error.

The level of significant	Confidence Interval
0.25	[0.200, 0.300]
0.20	[0.160, 0.240]
0.15	[0.120, 0.180]
0.10	[0.080, 0.120]
0.05	[0.040, 0.060]
0.01	[0.007, 0.015]

2) Set the number of treatments and replicates of experimental units in each treatment to be the same for every treatment. There were two cases, as shown in Table 3

Table 3 Sample size determination for various scenarios.

(n_1, n_2, n_3)	small	medium	large
equal	(10,10,10)	(30, 30, 30)	(100,100,100)
unequal	(5,10,15)	(25, 30, 35)	(95,100,105)

3) The treatment effect on the constant mean μ = 50 in two cases by Hasalems and Jitthavech [11].
a) When all values have the same mean.
b) When the means are not equal.

DOI: 10.60101/jarst.2023.251663

4) Set the distribution of errors (ε_i) to be normal with a specified mean and equal variance.

a) When the variance is the same for all populations, the variance ratio is 1:1:1.

b) When the variance is different for each population, three cases were studied.

Table 4 Ratio of variance classification of size.

Variance	Ratio
Small	1.5:2.4:3
Medium	1.5:6:9
Large	1.5:18:36

5) Randomly sample from the simulated data for each treatment with an equal number of replicates.

6) Test for equality of variances of the variable at a specified significance level of 0.05.

7) To compare the mean of 3 treatments from the hypothesis.

8) Repeat the above steps 5,000 times for each situation.

9) Compare the calculated test statistic value with the critical value using a specified significance level. Repeat this process 5,000 times for each situation to calculate the probability of Type I error and the power of the test.

10) Consider α_i in confidence interval as the Bradley's criteria when the nominal level is 0.05; if the calculated α_i falls within the criteria, it can be concluded that the test is able to control the probability of Type I error, and the penalized power of the three testing statistics can be calculated in the case where the test is able to control the probability of Type 1 error.

RESULTS AND DISCUSSIONS

This research is an experimental study to investigate and compare the efficiency of three test statistics for testing the mean of three populations, including the analysis of variance, (one-way ANOVA), Marascuilo Test, and the Mixed Bootstrap-Marascuilo Test. The results of the research can be summarized into two parts: 1. The ability to control the Type I error rate of the first Type of error using the Cochran criterion, and 2. Comparing the power of the tests. The symbols representing the test statistics are defined as follows:

F : One-Way ANOVA,
M : Marascuilo Test,
MBM: Mixed Bootstrap-Marascuilo Test.

The results of comparing the probability of Type I error rates are shown in Table 5 and Table 6. The results of comparing the power of the test are shown in Table 7 and Table 8.

Table 5 Probability of Type I error rate in the case of an equal sample size.

n_1, n_2, n_3	$\sigma_1^2, \sigma_2^2, \sigma_3^2$	Test		
		F	M	MBM
10,10,10	1:1:1	0.0516	0.0522	0.0502
	1.5:2.4:3	0.0526	0.0540	0.0554
	1.5:6:9	0.0584	0.0576	0.0560
	1.5:18:36	0.0644	0.0534	0.0494
30,30,30	1:1:1	0.0464	0.0492	0.0514
	1.5:2.4:3	0.0496	0.0530	0.0500
	1.5:6:9	0.0524	0.0500	0.0512
	1.5:18:36	0.0584	0.0510	0.0486
100,100,100	1:1:1	0.0510	0.0500	0.0464
	1.5:2.4:3	0.0506	0.0514	0.0410
	1.5:6:9	0.0526	0.0490	0.0492
	1.5:18:36	0.0582	0.0496	0.0536

Note: The underline indicates that the Type I error rate cannot be controlled by the Cochran criterion.

Table 6 Probability of Type I error rate in the case of unequal sample size.

n_1, n_2, n_3	$\sigma_1^2, \sigma_2^2, \sigma_3^2$	Test		
		F	M	MBM
5,10,15	1:1:1	0.0482	0.0574	0.0612
	1.5:2.4:3	0.0618	0.0566	0.0694
	1.5:6:9	0.0650	0.0544	0.0612
	1.5:18:36	0.0628	0.0558	0.0640
25,30,35	1:1:1	0.0500	0.0498	0.0484
	1.5:2.4:3	0.0450	0.0516	0.0500
	1.5:6:9	0.0454	0.0544	0.0496
	1.5:18:36	0.0452	0.0568	0.0532
95,100,105	1:1:1	0.0488	0.0474	0.0492
	1.5:2.4:3	0.0482	0.0486	0.0518
	1.5:6:9	0.0530	0.0526	0.0584
	1.5:18:36	0.0564	0.0520	0.0458

Note: The underline indicates that the Type I error rate cannot be controlled by the Cochran criterion.

Table 7 Power of the test in equal sample size.

n_1, n_2, n_3	$\sigma_1^2, \sigma_2^2, \sigma_3^2$	Test		
		F	M	MBM
10,10,10	1:1:1	0.13978	0.1391	0.1614
	1.5:2.4:3	0.09048	0.0904	0.0904
	1.5:6:9	0.06588	0.0695	0.0699
	1.5:18:36	-	0.0561	0.0512
30,30,30	1:1:1	0.3738	0.3849	0.4008
	1.5:2.4:3	0.1795	0.1882	0.1962
	1.5:6:9	0.0973	0.1108	0.1101
	1.5:18:36	0.0685	0.0743	0.0608
100,100, 100	1:1:1	0.8816	0.8876	0.8565
	1.5:2.4:3	0.5330	0.5503	0.4840
	1.5:6:9	0.2418	0.3054	0.2591
	1.5:18:36	0.0999	0.1219	0.1003

Note: The underline indicates the maximum power of the test.

DOI: 10.60101/jarst.2023.251663

Table 8 Power of the test in the case of unequal sample sizes.

n_1, n_2, n_3	$\sigma_1^2, \sigma_2^2, \sigma_3^2$	Test		
		F	M	MBM
5,10,15	1:1:1	0.1116	0.1167	-
	1.5:2.4:3	-	0.0876	-
	1.5:6:9	-	0.0669	-
	1.5:18:36	-	0.0530	-
25,30,35	1:1:1	0.3728	0.3705	0.3737
	1.5:2.4:3	0.1547	0.1918	0.1918
	1.5:6:9	0.0852	0.1239	0.1010
	1.5:18:36	0.0537	0.0696	0.0630
95,100,105	1:1:1	0.8799	0.8675	0.8905
	1.5:2.4:3	0.5313	0.5626	0.5170
	1.5:6:9	0.2211	0.2952	0.2376
	1.5:18:36	0.0943	0.1257	0.0987

Note: The underline indicates the maximum Power of the test.

The analysis of variance for a single-factor design can control the Type I error rate in all cases when the sample sizes are the same. This finding is consistent with the research conducted by Hasalems and Jitthavech [11].

The Marascuilo Test can control the Type I error rate and has the highest power when the population variances differ greatly. This is in line with the research results reported by Komduan [1].

Table 9 Test statistics that can control the Type I error rate probability.

n_1, n_2, n_3	$\sigma_1^2, \sigma_2^2, \sigma_3^2$			
	1:1:1	1.5:2.4:3	1.5:6:9	1.5:18:36
5,10,15	F, M	M	M	M
10,10,10	F, M, MBM	F, M, MBM	F, M, MBM	M, MBM
25,30,35	F, M, MBM	F, M, MBM	F, M, MBM	F, M, MBM
30,30,30	F, M, MBM	F, M, MBM	F, M, MBM	F, M, MBM
95,100,105	F, M, MBM	F, M, MBM	F, M, MBM	F, M, MBM
100,100,100	F, M, MBM	F, M, MBM	F, M, MBM	F, M, MBM

CONCLUSION

The analysis of variance with one-way can control the Type I error rate probability of Type I errors in almost all cases except when the sample size is the same and small (10, 10, 10) with significantly different variances (1.5:18:36) and when the sample size is different and small (5, 10, 15) with significantly different variances in all cases. The Marascuilo Test can control the Type I error rate probability of Type I errors in all cases, and the Mixed Bootstrap-Marascuilo Test can control the Type I error rate probability of Type I errors in almost all cases, except for the case of a small sample size (5, 10, 15) with different variances for all variances, as shown in Table 9. According to the results, the Mixed Bootstrap-Marascuilo test has the greatest testing ability in situations where there are equal small sample sizes with equal and moderate variances, as well as medium sample sizes with equal and small variances. Additionally, it shows an unequally large sample size with equal and large variances, as shown in Table10. This research can be used by organizations or researchers to select appropriate test statistics that are suitable for the characteristics of the data, both in cases where variances are equal and unequal and sample sizes are equal and unequal. In future research, the efficiency of test statistics for testing the equality of other means should be studied. This study used sample size, variance, and the influence of treatment factors that affect the ability to control Type I error and test power in only some cases, not all types of data. Therefore, in the future, the characteristics of data in different scenarios should be studied in more detail.

Table 10 The comparison of the power of the tests.

n_1, n_2, n_3	$\sigma_1^2, \sigma_2^2, \sigma_3^2$			
	1:1:1	1.5:2.4:3	1.5:6:9	1.5:18:36
5,10,15	M	M	M	M
10,10,10	MBM	F	MBM	M
25,30,35	MBM	MBM	M	M
30,30,30	MBM	MBM	M	M
95,100,105	MBM	M	M	MBM
100,100,100	M	M	M	M

REFERRENCES

1. Komduan J. Comparing the efficiency of mean testing statistics for three populations. [Master's thesis]. Bangkok: Faculty of Science King Mongkut's Institute of Technology Ladkrabang;2017.
2. Hananurak P. Comparing the Wilcoxon rank-sum test and the Mann-Whitney U test for testing population means with unequal variances. [Master's thesis]. Bangkok: Kasetsart University; 2006.
3. Efron B, Tibshirani RJ. An introduction to the bootstrap. 1st ed. New York: Chapman and Hall/CRC;1993.
4. Sangthong M. Nonparametric Bootstrap Method for Location Testing between Two Populations under Combined Assumption Violations. Burapha Science Journal. 2020;25(3):864-79.

DOI: 10.60101/jarst.2023.251663

5. Reiczigel J, Zakarias I, Rozsa L. A Bootstrap test of stochastic equality of two populations. The American Statistician. 2005;59:156-61.
6. Dag O, Dolgun A, Konar NM. Onewaytests: An R Package for One-Way Tests in Independent Groups Designs. R Journal. 2018;10(1):175-99.
7. Cavus M, Yazici B. Testing the equality of normal distributed and independent groups' means under unequal variances by doex package. The R Journal. 2021;12(2):134-54.
8. Marascuilo LA. Statistical for behavioral science research. New York: McGraw-Hill Book Co;1971.
9. Bradley JV. Robustness. Br J Math Stat Psychol. 1978;31(2):144-52.
10. Cavus M, Yazici B, Sezer A. Penalized power approach to compare the power of the tests when Type I error probabilities are different. Commun Stat - Simul Comput. 2021;50(7):1912-26.
11. Hasalems P, Jitthavech J. Comparing mean testing under variance heterogeneity in complete randomized experiments. Burapha Science Journal. 2018;23(1):135-45.

DOI: 10.60101/jarst.2023.251663

Received: March 14, 2023 | Revised: July 17, 2023 | Accepted: July 18, 2023

JOURNAL OF APPLIED RESEARCH ON SCIENCE AND TECHNOLOGY
JARST
INSTITUTE OF RESEARCH AND DEVELOPMENT
RAJAMANGALA UNIVERSITY OF TECHNOLOGY THANYABURI
ISSN ONLINE: 2773-9473
https://ph01.tci-thaijo.org/index.php/rmutt-journal

Further investigation on fixed point theorems via C-class functions in extended b-metric spaces

Tiwabhorn Khanpanuk* **and Chainarong Khunpanuk**

Mathematics and Computing Science Program, Faculty of Science and Technology, Phetchabun Rajabhat University, Phetchabun 67000, THAILAND

*Corresponding author: tiwabhorn.kha@pcru.ac.th

ABSTRACT

The purpose of this research project is to develop new theories, discuss, and extend some recent common fixed point results established when the underlying ambient space is an extended b-metric space and the contraction condition involves a new class of ψ-φ-C-contraction type mappings where ψ is the altering distance function and φ is the ultra-altering distance function. The unique fixed point theorems for such mappings in the setting of ψ-φ-complete metric spaces are proven. We also prove the fixed point theorem in partially ordered metric spaces. Moreover, some examples supporting the main results are given. Our results extend and generalize corresponding results in the literature. The start of the development of the theory of fixed points is tied to the end of the 19th century. The method of successive approximations is used in order to prove the solution's existence and uniqueness at the beginning of differential and integral equations. This branch of nonlinear analysis has been developed through various classes of spaces, such as metric spaces, topological spaces, probabilistic metric spaces, fuzzy metric spaces, and others. In developing the theory of fixed points, achievements are applied in various sciences, such as optimization, economics, and approximation theory. A very important step in the development of fixed point theory was taken by A.H. Ansari through the introduction of a C-class function. Using C-class functions, we generalize some known fixed point results, and Kamran et al. introduced a new intuitive concept of distance measure to extend the notion of b-metric space by further weakening the triangle inequality.

Keywords: fixed point, extended b-metric space, C-class function

INTRODUCTION

It is widely known that Thailand has a strategy to develop the nation using science and technology, particularly in applying scientific understanding to biotechnology, materials science technology, and suitable use of electronic and computer technology. Therefore, acquiring information is crucial for academic success, and it is evident that mathematics is an essential instrument for discovering and growing those above. Using knowledge of mathematics to create a mathematical model to predict the effect of soil temperature on plant growth, for example, In 2020, Boonwan J, et al. [3] created a mathematical model to predict soil temperature for the growth of chrysanthemum sprouts. However, fixed point theory is another tool used to solve many nonlinear problems in mathematical analysis. In 1922, Stefan Banach [17] began modern functional analysis and subsequently studied how to extend this principle for generalized contraction transmission in many different ways. Later, many researchers extended metric spaces to generalize metric spaces such as partial, G-metric, and cone metric spaces. For fixed point theorems in metric spaces, see [2, 4, 6, 10-13, 15, 16] and references therein. The concept of a b-metric space was introduced by Bakhtin [7], and Czerwik [9] generalized the structure of metric space by weakening the triangle inequality called a b-metric space and proved some results of the fixed point theorem in b-metric spaces. Further, many authors use the concepts for trade measures [5] and to measure ice floes [8]. In this context, Kamran and his co-authors [14] introduced the concept of extended b-metric space by further weakening the triangle inequality. Later in 2014, Ansari [1] introduced the concept of C-class functions and proved the unique fixed point theorems for specific contractive mappings concerning the C-class functions.

Following the above results, the motivation of this paper is to introduce the article's idea on some fixed point theorems for C-class functions in b-metric

J Appl Res Sci Tech 2023;22(2):251308

DOI: 10.60101/jarst.2023.251308

spaces [18] to cover more general cases. We then prove the existence of unique fixed points in extended b-metric space. Further, some examples supporting the main results are given.

MATERIALS AND METHODS

This section has compiled definitions and relevant theorems, a tool for further study and research in the main results.

Definition 2.1. [14] Let X be a nonempty set and $\theta: X \times X \rightarrow [1,\infty)$. A function $d_\theta: X \times X \rightarrow [1,\infty)$ is called an extended b metric space, if for all $x,y,z \in X$, it satisfies

EbM 1. $d_\theta(x,y) = 0$ if and only if $x=y$

EbM 2. $d_\theta(x,y) = d_\theta(y,x)$

EbM 3. $d_\theta(x,z) \leq \theta(x,z)[d_\theta(x,y) + d_\theta(y,z)]$

(X, d_θ) is called an extended b-metric space.

To show the concreteness of the idea of extended b-metric space, we give some examples of extended b-metric space in the following:

Example 2.2. Let $X = \{3,4,5\}$, $\theta: X \times X \rightarrow R^+$ and $d_\theta: X \times X \rightarrow R^+$ as $\theta(x,y) = x + y$

$d_\theta(3,3) = d_\theta(4,4) = d_\theta(5,5) = 0,$

$d_\theta(3,4) = d_\theta(4,3) = 50,$

$d_\theta(3,5) = d_\theta(5,3) = 250,$

$d_\theta(4,5) = d_\theta(5,4) = 400.$

It is obvious from definition 2.1 in EbM 1. and EbM 2. We then prove EbM 3. in the following way:

$50 = d_\theta(3,4) \leq \theta(3,4)[d_\theta(3,5) + d_\theta(5,4)] = 4{,}550$

$250 = d_\theta(3,5) \leq \theta(3,5)[d_\theta(3,4) + d_\theta(4,5)] = 3{,}600$

$450 = d_\theta(4,5) \leq \theta(4,5)[d_\theta(4,3) + d_\theta(3,5)] = 2{,}700$

Therefore, (X, d_θ) is an extended b-metric space.

Example 2.3. [14] Let $X = [0, +\infty)$ and $\theta: X \times X \rightarrow [1, +\infty)$, $\theta(x,y) = 1 + x + y$.

Define $d_\theta: X \times X \rightarrow [1, +\infty)$, as

$d_\theta(x,y) = x + y$, for $x, y \in X, x \neq y$

$d_\theta(x,y) = 0$, for $x, y \in X, x = y$.

It is easy to show EbM1. and EbM 2. Hold. For EbM 3. We split the consideration into four cases:

Case 1. If $x = y$, we have EbM 3. hold.

Case 2. If $x \neq y, x = z$, then

$\theta(x,y)\,[d_\theta(x,z) + d_\theta(z,y)]$

$= (1 + x + y)[0 + (z + y)]$

$= (1 + x + y)(z + y)$

$\geq x + y = d_\theta(x,y).$

Case 3. If $x \neq y, y = z$, then

$\theta(x,y)[d_\theta(x,z) + d_\theta(z,y)]$

$= (1 + x + y)[(x + z) + 0]$

$= (1 + x + y)(x + y)$

$\geq x + y = d_\theta(x,y)$

Case 4. If $x \neq y, y \neq z, x \neq z$, then

$\theta(x,y)[d_\theta(x,z) + d_\theta(z,y)]$

$= (1 + x + y)[(x + z) + (z + y)]$

$\geq x + 2z + y$

$\geq x + y = d_\theta(x,y).$

In conclusion, for any $x, y, z \in X$,

$d_\theta(x,z) \leq \theta(x,z)[d_\theta(x,y) + d_\theta(y,z)].$

Hence, (X, d_θ) is an extended b metric space.

In the next section, the concepts of convergence, Cauchy sequence, and completeness are introduced in extended b-metric space.

Definition 2.4. [14] Let (X, d_θ) be an extended b-metric space. Then a sequence (x_n) in X is said to be:

1) **convergent** if and only if there exists $x \in X$ such that $\lim_{n\rightarrow\infty} x_n = x,$

2) **Cauchy** if and only if $\lim_{m,n\rightarrow\infty} d_\theta(x_m, x_n) = 0.$

Definition 2.5. An extended b metric space. (X, d_θ) is complete if every Cauchy sequence in X is convergent.

Lemma 2.6. Let (X, d_θ) be a complete extended b-metric space. If d_θ is continuous, then every convergent sequence has a unique limit.

Definition 2.7. [1] A mapping $F: [0,\infty)^2 \rightarrow R$ is called a C-class function if it is continuous and for all $a, b \in [0,\infty)$

1) $F(a,b) \leq a$;

2) $F(a,b) = a$ implies that either $a = 0$ or $b = 0$.

We denote C as the family set of all C-class functions.

Example 2.8. [1] The following functions $F: [0,\infty)^2 \rightarrow R^2$ are elements in C. For all $a, b \in [0,\infty)$

1) $f(a,b) = a - b, f(a,b) = a \rightarrow b = 0;$

2) $f(a,b) = xa\,, f(a,b) = a \rightarrow a = 0$ where $0 < x < 1;$

3) $f(a,b) = (a + x)^{\left(\frac{1}{1+b}y\right)} - x, f(a,b) = a \rightarrow b = 0$ where $x > 1\,, y \in (0,\infty);$

4) $f(a,b) = \log\frac{b + x\,a}{1 + b}, x > 1,$

$(a,b) = a \Rightarrow a = 0$ or $b = 0;$

5) $f(a,b) = \ln(1 + xa)/2, x > e,$

$f(a,b) = a \Rightarrow a = 0;$

6) $f(a,b) = a\,(1 + b)\,x; x \in (0,\infty),$

$f(a,b) = a \Rightarrow a = 0$ or $b = 0;$

7) $f(a,b) = a \log_{b+x} x, x > 1,$

$f(a,b) = a \Rightarrow a = 0$ or $b = 0;$

8) $f(a,b) = a - \left(\frac{1+a}{2+a}\right)\left(\frac{b}{1+b}\right),$

$f(a,b) = a \Rightarrow b = 0\,;$

9) $f(a,b) = a; \beta(a), \beta: [0,\infty) \rightarrow [0,1)$ is continuous

$f(a,b) = a \Rightarrow a = 0;$

10) $f(a,b) = a - \frac{b}{k+b}, f(a,b) = a \Rightarrow b = 0;$

11) $f(a,b) = a - \varphi(a), f(a,b) = a \Rightarrow a = 0,$

$\varphi: [0,\infty) \rightarrow [0,\infty)$ is a continuous function such that $\varphi(t) = 0 \rightarrow t = 0;$

12) $f(a,b) = ah(a,b), f(a,b) = a \Rightarrow a = 0$

$h: [0,\infty) \times [0,\infty) \rightarrow [0,\infty)$ is a continuous function such that $h(b,a) < 1$ for all $b, a > 0;$

13) $f(a,b) = a - \left(\frac{2-b}{1+b}\right) b\,, f(a,b) = a \Rightarrow a = 0;$

14) $f(a,b) = \sqrt[n]{\ln(1 + a^n)}\,, f(a,b) = a \Rightarrow a = 0;$

15) $f(a,b) = \varphi(a), f(a,b) = a \Rightarrow a = 0$

$\varphi: [0,\infty) \rightarrow [0,\infty)$ is a continuous function such that $\varphi(0) = 0$ and $\varphi(b) < b$ for $b > 0;$

16) $f(a,b) = \frac{a}{(1+a)^x}, x \in (0,\infty),$

$f(a,b) = a \Rightarrow a = 0.$

DOI: 10.60101/jarst.2023.251308

Definition 2.9. [1] $\psi : [0,\infty) \to [0,\infty)$ is called an altering distance function if the following properties are satisfied:
1) ψ is non-decreasing and continuous;
2) $\psi(t) = 0$ if and only if $t = 0$.
The family of all altering distance functions is denoted by ψ.

Example 2.10. The following functions
$\psi_i : R^+ \to R^+, i \in \{1,2,3,\dots,6\}$ are elements in ψ
1) $\psi_1(x) = kx$ where $k > 0$,
2) $\psi_2(x) = x^\alpha$ where $\alpha > 0$,
3) $\psi_3(x) = \sinh^{-1} x$,
4) $\psi_4(x) = \cosh x - 1$,
5) $\psi_5(x) = a^x - 1$ where $0 < a \neq 1$.

Definition 2.11. [1] A function $\varphi : [0,\infty) \to [0,\infty)$ is called an ultra-altering distance function if the following properties are satisfied in the following
1) φ is continuous;
2) $\varphi(t) > 0$ if and only if $t > 0$.
We denoted Ψu as the family of all ultra-altering distance functions.

RESULTS AND DISCUSSION

In this section, we are now ready to prove our main results.

Theorem 3.1. Let a function $d_\theta : X \times X \to [0,\infty)$ is an extended b metric space, and $f : X \to X$ is a self-mapping. Suppose

$$\psi\left(\theta(x,y)d_\theta\left(f_x, f_y\right)\right)$$
$$\leq F(\psi(M(x,y)), \phi(M(x,y))) + LN(x,y) \qquad (3.1)$$

for all $x, y \in X$, where $L \geq 0, F : [0,\infty)^2 \to R$ is an element in C, $\psi : [0,\infty) \to [0,\infty)$ is an element in Ψ, $\varphi : [0,\infty) \to [0,\infty)$ is an element in Ψu and

$$M(x,y) = \max\left\{d_\theta(x,y), \frac{d_\theta(x,f_x)d_\theta(y,f_y)}{1+d_\theta(f_x,f_y)}\right\} \text{ and}$$

$$N(x,y) = \min\{d_\theta(x,f_x), d_\theta\left(x,f_y\right), d_\theta(y,f_x), d_\theta\left(y,f_y\right)\}.$$

Then f has a unique fixed point.

Proof. Let $x_0 \in X$. Define a sequence $(x_n) \subset X$ by $x_n = f^n(x_0) = fx_{n-1}$ for $n \in N \cup \{0\}$. We now prove that (x_n) is a Cauchy sequence. First, we show $\lim\limits_{n\to\infty} d_\theta(x_n, x_{n+1}) = 0$.

From 3.1 we have,

$$d_\theta(x_n, x_{n+1}) \leq \theta(x_n, x_{n+1})d_\theta(x_n, x_{n+1})$$
$$= \theta(x_n, x_{n+1})d_\theta(f(x_{n-1}), f(x_n)).$$

Consequently $\psi d_\theta(x_n, x_{n+1})$

$$\leq \psi(\theta(x_n, x_{n+1})d_\theta(f(x_{n-1}), f(x_n))$$
$$\leq F(\psi(M(x_{n-1}, x_n)), \varphi(M(x_{n-1}, x_n)))$$
$$+ LN(x_{n-1}, x_n) \qquad (3.2)$$

where $M(x_{n-1}, x_n)$

$$= \max\left\{d_\theta(x_{n-1}, x_n), \frac{d_\theta(x_{n-1}, fx_{n-1})d_\theta(x_n, fx_n)}{1 + d_\theta(fx_{n-1}, fx_n)}\right\}$$
$$= \max\left\{d_\theta(x_{n-1}, x_n), \frac{d_\theta(x_{n-1}, x_n)d_\theta(x_n, x_{n-1})}{1 + d_\theta(x_n, x_{n+1})}\right\}$$
$$= d_\theta(x_{n-1}, x_n)$$

and $N(x_{n-1}, x_n)$

$$= \min\{d_\theta(x_{n-1}, fx_{n-1}), d_\theta(x_{n-1}, fx_n), d_\theta(x_n, fx_{n-1}), d_\theta(x_n, fx_n)\}$$
$$= \min\{d_\theta(x_{n-1}, x_n), d_\theta(x_{n-1}, x_{n+1}), d_\theta(x_n, x_n), d_\theta(x_n, x_{n+1})\}$$
$$= \min\{d_\theta(x_{n-1}, x_n), d_\theta(x_{n-1}, x_{n+1}), 0, d_\theta(x_n, x_{n+1})\}$$
$$= 0.$$

Therefore, it follows from 3.2 that we have

$$\psi(\theta(x_n, x_{n+1})d_\theta(f(x_{n-1}), f(x_n))$$
$$\leq F(\psi(d_\theta(x_{n-1}, x_n)), \varphi(d_\theta(x_{n-1}, x_n)) + LN(x_{n-1}, x_n)$$
$$= F(\psi(d_\theta(x_{n-1}, x_n)), \varphi(d_\theta(x_{n-1}, x_n)) + L(0)$$
$$= F(\psi(d_\theta(x_{n-1}, x_n)), \varphi(d_\theta(x_{n-1}, x_n))$$

thus

$$\psi(d_\theta(x_n, x_{n+1}) \leq F(\psi\big(d_\theta(x_{n-1}, x_n)\big),$$
$$\varphi\big(d_\theta(x_{n-1}, x_n)\big)\big). \qquad (3.3)$$

Since F is a function in C, we have

$$\psi(d_\theta(x_n, x_{n+1})$$
$$\leq F(\psi(d_\theta(x_{n-1}, x_n)), \varphi(d_\theta(x_{n-1}, x_n))$$
$$\leq \psi\big(d_\theta(x_{n-1}, x_n)\big) \qquad (3.4)$$
$$= \psi\big(d_\theta(x_n, x_{n-1})\big)$$

And ψ is non-decreasing, thus
$d_\theta(x_n, x_{n+1}) \geq 0 \; \forall n \in N$.
And $\{d_\theta(x_n, x_{n+1})\}$ is a descending sequence.
Then it converges, and there exists $r \geq 0$ such that $\lim\limits_{n\to\infty} d_\theta(x_n, x_{n+1}) = r$.
Let $n \to \infty$, then from 3.4 it implies that

$$\psi(r) = \psi \lim_{n\to\infty} d_\theta(x_n, x_{n+1}) \leq \psi(x_n, x_{n-1})$$
$$= \lim_{n\to\infty} \psi(d_\theta(x_n, x_{n+1})) \leq \psi \lim_{n\to\infty} d_\theta(x_{n-1}, x_n)$$
$$\leq \lim_{n\to\infty} F(\psi(d_\theta(x_{n-1}, x_n)) , \varphi(d_\theta(x_{n-1}, x_n)) \leq \psi(r)$$
$$= F \lim_{n\to\infty} (\psi(d_\theta(x_{n-1}, x_n)) , \varphi(d_\theta(x_{n-1}, x_n)) \leq \psi(r)$$
$$= F(\psi(\lim_{n\to\infty}((d_\theta(x_{n-1}, x_n))) , (\varphi(\lim_{n\to\infty}((d_\theta(x_{n-1}, x_n)))$$
$$\leq \psi(r)$$
$$= F(\psi(r), \varphi(r)) \leq \psi(r)$$

therefore $r = 0$ and $\lim\limits_{n\to\infty} d_\theta(x_{n-1}, x_n) = 0$. (3.5)

Next, it is proved that the sequence (x_n) is a Cauchy sequence. Suppose that (x_n) is not a Cauchy sequence. By definition 2.4, we have $\varepsilon > 0$, for which we can find two sequences of positive integers $(m(k))$ and $(n(k))$ such that for all positive integers $k, n(k) > m(k) > k$ and $d\big(x_{m(k)}, x_{n(k)}\big) \geq \varepsilon$. Let $n(k)$ be the smallest such positive integer $n(k) > m(k) > k$ such that $\forall k \in I^+$

$$d_\theta\big(x_{m(k)}, x_{n(k)}\big) \geq \varepsilon,$$
$$d\big(x_{m(k)}, x_{n(k)-1}\big) > \varepsilon \qquad (3.6)$$

by 3.6 and $\theta : X \times X \to [1,\infty)$
we have

$$\liminf_{n\to\infty} (\varepsilon) \leq \liminf_{n\to\infty} (d_\theta\big(x_{m(k)}, x_{n(k)-1}\big))$$
$$\varepsilon \leq \liminf_{n\to\infty} (d_\theta\big(x_{m(k)}, x_{n(k)-1}\big)) \qquad (3.7)$$
$$\theta(x_{m(k)}, x_{n(k)-1}) \geq 1. \qquad (3.8)$$

Since 3.7 and 3.8, we have

$$0 < \frac{\varepsilon}{\theta(x_{m(k)}, x_{n(k)-1})} \leq \varepsilon$$
$$\leq \liminf_{n\to\infty} (d_\theta\big(x_{m(k)}, x_{n(k)-1}\big))$$

where $M\big(x_{m(k)}, x_{n(k)-1}\big)$

$$= \max\{d_\theta\big(x_{m(k)}, x_{n(k)-1}\big),$$

DOI: 10.60101/jarst.2023.251308

$$\frac{d_\theta\left(x_{n(k)-1}, fx_{n(k)-1}\right)d_\theta\left(x_{m(k)}, fx_{m(k)}\right)}{1+d_\theta\left(fx_{n(k)-1}, fx_{m(k)}\right)}\}$$

$$= \max\{d_\theta\left(x_{m(k)}, x_{n(k)-1}\right), \frac{d_\theta\left(x_{n(k)-1}, x_{n(k)}\right)d_\theta\left(x_{m(k)}, x_{m(k)+1}\right)}{1+d_\theta\left(x_{n(k)}, x_{m(k)+1}\right)}\}.$$

Let $k \to \infty$ and apply 3.4, 3.5, and 3.6. We get

$$\frac{\varepsilon}{\theta^2 x_{m(k)}, x_{n(k)-1}} \leq \lim_{k\to\infty} \inf f\left(M\left(x_{m(k)}, x_{n(k)-1}\right)\right). \qquad (3.9)$$

Also $\lim_{k\to\infty} N\left(x_{m(k)}, x_{n(k)-1}\right)$

$$= \lim_{k\to\infty} \min\{d_\theta\left(x_{n(k)-1}, fx_{n(k)-1}\right), d_\theta\left(x_{m(k)}, fx_{m(k)-1}\right), d_\theta\left(x_{n(k)}, fx_{m(k)}\right)\}$$

$$= \min\{\lim_{k\to\infty} d_\theta\left(x_{n(k)-1}, x_{n(k)}\right), \lim_{k\to\infty} d_\theta\left(x_{m(k)}, x_{m(k)+1}\right), \lim_{k\to\infty} d_\theta\left(x_{n(k)}, x_{m(k)+1}\right), \lim_{k\to\infty} d_\theta\left(x_{m(k)}, x_{m(k)}\right)\}$$

$$= \min\{\lim_{k\to\infty} d_\theta\left(x_{n(k)-1}, x_{n(k)}\right), \lim_{k\to\infty} d_\theta\left(x_{m(k)}, x_{m(k)+1}\right), \lim_{k\to\infty} d_\theta\left(x_{m(k)}, x_{m(k)}\right)\}$$

$$= 0.$$

Then

$$d_\theta\left(x_{m(k)}, x_{n(k)}\right) - \theta(x_{m(k)}, x_{n(k)})d_\theta\left(x_{m(k)}, x_{m(k)+1}\right)$$
$$\leq \theta\left(x_{m(k)}, x_{n(k)}\right)d_\theta\left(x_{m(k)+1}, x_{n(k)}\right). \qquad (3.10)$$

from 3.7 and 3.9 we get

$$\psi(\varepsilon) \leq \psi(\lim_{k\to\infty} \sup d_\theta(x_{m(k)}, x_{n(k)}))$$
$$\leq \psi(\lim_{k\to\infty} \sup d_\theta(x_{m(k)}, x_{n(k)}))d_\theta(x_{m(k)+1}, x_{n(k)})$$
$$\leq F(\psi\left(\lim_{k\to\infty} \sup M\left(x_{m(k)}, x_{n(k)-1}\right)\right),$$
$$\varphi(\left(\lim_{k\to\infty} \inf M\left(x_{m(k)}, x_{n(k)-1}\right)\right))$$
$$\leq \psi(\varepsilon)$$

and $F\left(\psi(\varepsilon), \varphi\left(\lim_{k\to\infty} \inf M(x_{m(k)}, x_{n(k)-1}\right)\right) = \psi(\varepsilon)$. by definition 2.7 2) we get $\psi(\varepsilon) = 0$ or

$$\varphi\left(\lim_{k\to\infty} \inf M(x_{m(k)}, x_{n(k)-1}\right) = 0$$

and by definition 2.9 2) we get $\varepsilon = 0$ or

$$\lim_{k\to\infty} \inf M(x_{m(k)}, x_{n(k)-1} = 0.$$

it is a contradiction with $\varepsilon > 0$ and

$$\lim_{k\to\infty} \inf (M\left(x_{m(k)}, x_{n(k)-1}\right)) \geq \frac{\varepsilon}{d_\theta\left(x_{m(k)}, x_{n(k)}\right)^2}$$

thus (x_n) is an extended b-Cauchy sequence in X. Since (X, d) is a completely extended b metric space, there exists $u \in X$ such that $\lim_{n\to\infty} x_n = u$ now, we show u is a fixed point of f since

$$1 \leq \theta(u, fu) \text{ and } d_\theta(u, fu) \geq 0$$

we get $d_\theta(u, fu) \leq \theta(u, fu)d_\theta(u, fu)$.

And since ψ is a nondecreasing function implies

$$\psi(d_\theta(u, fu)) \leq \psi(\theta(u, fu)d_\theta(u, fu)) \qquad (3.11)$$

$$\psi(\theta(u, fu)d_\theta(f\left(\lim_{n\to\infty} x_n, f(\lim_{n\to\infty} x_n\right))$$
$$= \psi(\theta(u, fu)(d_\theta fu, f(fu)))$$
$$= \psi(\theta(u, fu)d_\theta(u, fu))\psi(\theta(u, fu)\theta(u, fu)(u, fu))$$
$$\leq F(\psi(M(u, fu)), \varphi(M(u, fu))) + LN(u, fu) \qquad (3.12)$$

but $M(u, fu) = d_\theta(u, fu)$ and $N(u, fu) = 0$ thus

$$\psi(d(u, f(u))) \leq F\,\psi(\theta(u, f(u))), \varphi d(u, f(u)$$
$$\leq \psi(d(u, f(u)))$$

So $\psi(d(u, f(u))) = F\,\psi(\theta(u, f(u))), \varphi d(u, f(u))$.

$\therefore\ \psi(\theta(u, f(u))) = 0$ or $\varphi d(u, f(u)) = 0$.

By definition 2.1 we have $d(u, f(u)) = 0$ so $u = f(u)$

Now, we will show that u is a unique fixed point of f. Suppose $v \neq u$ is another fixed point of f from 3.1. We have

$$\psi(d(u, f(u))) \leq \psi(\theta(u, v), d(u, v))$$
$$= \psi(\theta(u, v), d(f(u), f(v))$$
$$\leq F(\psi(M(u, v)), \varphi M(u, v)) + LN(u, v)$$
$$\leq F(\psi(M(u, v)), \varphi M(u, v))$$
$$\leq F(\psi(d(u, v)), \varphi d(u, v))$$
$$\leq \psi(d(u, v))$$

so $\psi d(u, v) = F(\psi(d(u, v), \varphi\, d(u, v))$

thus $\psi(d(u, v) = 0$ or $\varphi d(u, v) = 0$.

By definition 2.9, we have $d(u, v) = 0$ so that $u = v$ It means that f has a unique fixed point.

Example 3.2. Let $d_\theta: X \times X \to R^+$ and (X, d_θ) is an extended b metric space. $f: X \to X$ be such that $f(x) = \frac{x}{2}$, $\theta: X \times X \to R^+$ satisfy

$$\theta(x, y) = \begin{cases} |x-y|^3 & ; x \neq y \\ 1 & ; x = y \end{cases}$$

And define $F: [0, \infty)^2 \to R^2$ by $F(x, y) = x - y$ and define $\psi: [0, \infty) \to [0, \infty)$, $\varphi: [0, \infty) \to [0, \infty)$ by $\psi(x) = 2x$ and $\varphi(x) = x$ respectively.

$M(x, y) = \max\{ d_\theta(x, y), \frac{d_\theta(x,fx)d_\theta(y,fy)}{1+d_\theta(fx,fy)}\}$ and

$N(x, y) = \min\{d_\theta(x, fx), d_\theta(x, fy), d_\theta(y, fx), d_\theta(y, fy)\}$.

From, example 2.8, definition 2.9, and definition 2.11 invoke that F is in C,ψ is in Ψ, and φ is in Ψu. Next, it will be considered that

$$\psi\left(\theta(x, y)d_\theta(fx, fy)\right)$$
$$\leq F(\psi(M(x, y)), \varphi(M(x, y))) + LN(x, y).$$

It will be considered in 3 cases: $x = y$, $x > y$ and $x < y$ as follows.

Case 1: if $x = y$

Since $x = y$ therefore that $\theta(x, y) = 1$ and

$d_\theta(x, y) = d_\theta(fx, fy) = 0$ and

$$d_\theta(x, fx) = d_\theta(y, fy) = d_\theta(x, fy) = d_\theta(y, fx)$$
$$= (x - \frac{x}{2})^4 = \frac{x^4}{16}.$$

So that $\frac{d_\theta(x,fx)d_\theta(y,fy)}{1+d_\theta(fx,fy)} = \frac{\left(\frac{x^4}{16}\right)^2}{1+0} = \frac{x^8}{256}$.

And consider that

$$M(x, y) = \max\left\{d_\theta(x, y), \frac{d_\theta(x,fx)d_\theta(y,fy)}{1+d_\theta(fx,fy)}\right\}$$
$$= \max\left\{0, \frac{x^8}{256}\right\} = \frac{x^8}{256} \quad \text{and}$$

$$N(x, y) = \min\{d_\theta(x, fx), d_\theta(x, fx), d_\theta(y, fx), d_\theta(y, fy)\}$$
$$= \frac{x^4}{16}.$$

Next, it will be considered that

$\psi(\theta(x, y)d_\theta(fx, fy))$ by $\theta(x, y) = 1$ and

$d_\theta(x, y) = d_\theta(fx, fy) = 0$. We have

$$\psi(\theta(x, y)d_\theta(fx, fy)) = \psi(1(0)) = \psi(0) = 0.$$

And $F(\psi(M(x, y)), \varphi(M(x, y))) + LN(x, y)$

$$\psi(M(x, y)) = \psi(\frac{x^8}{256}) = 2(\frac{x^8}{256}) = \frac{x^8}{128}$$

$\varphi(M(x, y)) = \varphi(\frac{x^8}{256}) = \frac{x^8}{256}$ then we have

$$F\left(\psi\left(M(x, y)\right), \varphi\left(M(x, y)\right)\right) = F\left(\frac{x^8}{128}, \frac{x^8}{256}\right) = \frac{x^8}{256}.$$

Hence $F(\psi(M(x, y)), \varphi(M(x, y))) + N(x, y)$

$= \frac{x^8}{256} + \frac{x^4}{16}$ such that $0 \le \frac{x^8}{256} + \frac{x^4}{16}$ so if $x = y$ then we have

$$\psi\big(\theta(x,y)d_\theta(fx,fy)\big)$$
$$\le F(\psi(M(x,y)), \varphi(M(x,y))) + N(x,y).$$

Case 2: $x > y$

Since $x > y$ then we have

$\theta(x,y) = |x-y|^3 = (x-y)^3$

and $d_\theta(x,y) = (x-y)^4$

$$d_\theta(x,fx) = \left(x - \frac{x}{2}\right)^4 = \frac{x^4}{16}$$

$$d_\theta(y,fy) = \left(y - \frac{y}{2}\right)^4 = \frac{y^4}{16}$$

$$d_\theta(x,fy) = \left(x - \frac{y}{2}\right)^4 = \frac{(2x-y)^4}{16}$$

$$d_\theta(y,fx) = \left(y - \frac{x}{2}\right)^4 = \frac{(2y-x)^4}{16}$$

$$d_\theta(fx,fy) = \left(\frac{x}{2} - \frac{y}{2}\right)^4 = \frac{(x-y)^4}{16}.$$

Therefore $\frac{d_\theta(x,fx)d_\theta(y,fy)}{1+d_\theta(fx,fy)} = \frac{\left(\frac{x^4}{16}\right)\left(\frac{y^4}{16}\right)}{1+\left(\frac{(x-y)^4}{16}\right)} = \left(\frac{\frac{x^4y^4}{16}}{16+(x-y)^4}\right)$.

Next, it will be considered that

$$M(x,y) = \max\left\{d_\theta(x,y), \frac{d_\theta(x,fx)\,d_\theta(y,fy)}{1+d_\theta(fx,fy)}\right\}$$

$= \max\left\{(x-y)^4, \left(\frac{\frac{x^4y^4}{16}}{16+(x-y)^4}\right)\right\} = (x-y)^4$ and

$$N(x,y) = \min\{d_\theta(x,fx), d_\theta(x,fy), d_\theta(y,fx), d_\theta(y,fy)\}$$

$$= \min\left\{\frac{x^4}{16}, \frac{(2x-y)^4}{16}, \frac{(2y-x)^4}{16}, \frac{y^4}{16}\right\} = \frac{(2y-x)^4}{16}.$$

And $\psi(\theta(x,y)d_\theta(fx,fy))$ by $\theta(x,y) = |x-y|^3$

and $d_\theta(fx,fy) = \frac{(x-y)^4}{16}$

$$\psi(\theta(x,y)d_\theta(fx,fy)) = \psi(|x-y|^3 \frac{(x-y)^4}{16})$$

$$= \psi\left(\frac{(x-y)^7}{16}\right)$$

$$= \frac{(x-y)^7}{8}.$$

And next regard

$$F(\psi(M(x,y)), \varphi(M(x,y))) + N(x,y)$$

$$\psi(M(x,y)) = \psi((x-y)^4) = 2((x-y)^4)$$

$$\varphi(M(x,y)) = \varphi((x-y)^4) = (x-y)^4.$$

We have

$$F\big(\psi(M(x,y)), \varphi(M(x,y))\big)$$

$$= F(2(x-y)^4, (x-y)^4)$$

$$= 2(x-y)^4 - (x-y)^4 = (x-y)^4$$

So $F(\psi(M(x,y)), \varphi(M(x,y))) + N(x,y)$

$$= (x-y)^4 + \frac{(2y-x)^4}{16}$$

such that $\frac{(x-y)^7}{8} \le (x-y)^4 + \frac{(2y-x)^4}{16}$. Consequently, if $x > y$ we have

$$\psi\big(\theta(x,y)d_\theta(fx,fy)\big)$$
$$\le F(\psi(M(x,y)), \varphi(M(x,y))) + N(x,y).$$

Case 3: if $x < y$

Since $x < y$, we have

$\theta(x,y) = |x-y|^3 = -(x-y)^3$ and

$d_\theta(x,y) = (x-y)^4$

$$d_\theta(x,fx) = \left(x - \frac{x}{2}\right)^4 = \frac{x^4}{16}$$

$$d_\theta(y,fy) = \left(y - \frac{y}{2}\right)^4 = \frac{y^4}{16}$$

$$d_\theta(x,fy) = \left(x - \frac{y}{2}\right)^4 = \frac{(2x-y)^4}{16}$$

$$d_\theta(y,fx) = \left(y - \frac{x}{2}\right)^4 = \frac{(2y-x)^4}{16}$$

$$d_\theta(fx,fy) = \left(\frac{x}{2} - \frac{y}{2}\right)^4 = \frac{(x-y)^4}{16}.$$

Then $\frac{d_\theta(x,fx)d_\theta(y,fy)}{1+d_\theta(fx,fy)} = \frac{\left(\frac{x^4}{16}\right)\left(\frac{y^4}{16}\right)}{1+\left(\frac{(x-y)^4}{16}\right)} = \left(\frac{\frac{x^4y^4}{16}}{16+(x-y)^4}\right)$. Consider that

$$M(x,y) = \max\left\{d_\theta(x,y), \frac{d_\theta(x,fx)\,d_\theta(y,fy)}{1+d_\theta(fx,fy)}\right\}$$

$$N(x,y) = \min\{d_\theta(x,fx), d_\theta(x,fy), d_\theta(y,fx), d_\theta(y,fy)\}$$

$\max\left\{(x-y)^4, \left(\frac{\frac{x^4y^4}{16}}{16+(x-y)^4}\right)\right\} = (x-y)^4$ and

$$N(x,y) = \min\{d_\theta(x,fx), d_\theta(x,fy), d_\theta(y,fx), d_\theta(y,fy)\}$$

$$= \min\left\{\frac{x^4}{16}, \frac{(2x-y)^4}{16}, \frac{(2y-x)^4}{16}, \frac{y^4}{16}\right\} = \frac{(2y-x)^4}{16}$$

$\psi(\theta(x,y)d_\theta(fx,fy))$ by $\theta(x,y) = -(x-y)^3$

and $d_\theta(fx,fy) = \frac{(x-y)^4}{16}$

$$\psi(\theta(x,y)d_\theta(fx,fy)) = \psi(|x-y|^3 \frac{(x-y)^4}{16})$$

$$= \psi\left(\frac{-(x-y)^7}{16}\right)$$

$$= \frac{-(x-y)^7}{8}.$$

Next, it will be considered that

$F(\psi(M(x,y)), \varphi(M(x,y))) + N(x,y)$

$\psi(M(x,y)) = \psi((x-y)^4) = 2((x-y)^4)$

$\varphi\big(M(x,y)\big) = \varphi((x-y)^4) = (x-y)^4.$

Therefore $F(\psi(M(x,y)), \varphi(M(x,y)))$

$= F(2(x-y)^4, (x-y)^4)$

$= 2(x-y)^4 - (x-y)^4 = (x-y)^4.$

So $F(\psi(M(x,y)), \varphi(M(x,y))) + N(x,y)$

$$= (x-y)^4 + \frac{(2x-y)^4}{16}$$

such that $\frac{-(x-y)^7}{8} \le (x-y)^4 + \frac{(2x-y)^4}{16}$.

Consequently, if $x < y$ we have

$\psi\big(\theta(x,y)d_\theta(fx,fy)\big) \le F(\psi(M(x,y)), \varphi(M(x,y))) + N(x,y)$.

By the fact that $f(x) = \left(\frac{x}{2}\right)$, function f has a unique fixed point that is 0.

Corollary 3.3, let (X,d) be a complete extended b-metric space on X and $f: X \to X$ be self-mapping. If $\psi\big(\theta(x,y)d_\theta(fx,fy)\big) \le F(\psi(M(x,y)), \varphi(M(x,y))) + N(x,y)$. for all $x, y \in X$, where $\psi: [0,\infty) \to [0,\infty)$ is an ultra altering distance function and $M(x,y) = \max\left\{d_\theta(x,y), \frac{d_\theta(x,fx)\,d_\theta(y,fy)}{1+d_\theta(fx,fy)}\right\}$ and

$$N(x,y) = \min\{d_\theta(x,fx), d_\theta(x,fy), d_\theta(y,fx), d_\theta(y,fy)\}$$

then f has a unique fixed point.

Proof. Let $F(a,b) = a - b$. By example 2.8, we have F as a C-class function.
so $\psi\big(\theta(x,y)d_\theta(fx,fy)\big)$
$\leq \psi(M(x,y)) - \varphi(M(x,y)) + LN(x,y)$
$= F(\psi(M(x,y)), \phi(M(x,y))) + LN(x,y)$.
Thus all the conditions of theorem 3.1 are satisfied. Hence f has a unique fixed point.

Corollary 3.4, let (X,d) be a complete extended b-metric space on X and $f: X \to X$ be self-mapping. $\theta: X \times X \to [1,\infty)$. Suppose $\psi\big(\theta(x,y)d_\theta(fx,fy)\big)$
$\leq \psi\big(M(x,y)\big)\beta\psi(M(x,y) + LN(x,y))$.
for all $x,y \in X$, where $\beta: [0,\infty) \to [0,1)$ is continuous and
$M(x,y) = \max\left\{d_\theta(x,y), \frac{d_\theta(x,fx)\, d_\theta(y,fy)}{1+d_\theta(fx,fy)}\right\}$ and
$N(x,y) = \min\{d_\theta(x,fx), d_\theta(x,fy), d_\theta(y,fx), d_\theta(y,fy)\}$
then f has a unique fixed point.

Proof. Let $F(a,b) = \theta(x,y)\beta(a)$
where $\beta: [0,\infty) \to [0,1)$ is continuous.
And let $\psi(b) = b$ by corollary 3.3 we have
$\psi(\theta(x,y)d_\theta(fx,fy)$
$\leq \psi(M(x,y))\beta(\psi(M(x,y))) + LN(x,y)$
$= F(\psi(M(x,y)), \beta(\psi(M(x,y)))) + LN(x,y)$
Thus, all the conditions of theorem 3.1 are satisfied. Hence, f has a unique fixed point.

Corollary 3.5, let (X,d) be a complete extended b-metric space on X and $f: X \to X$
be self-mapping. $\theta: X \times X \to [1,\infty)$.
Suppose
$d\big(f(x),f(y)\big) \leq \left[\frac{\beta\left(M(x,y)\right)}{s}\right] M(x,y) + LN(x,y)$
for all $x,y \in X$, where $L \geq 0$,
$\beta: [0,\infty) \to [0,1)$ is continuous. And
$M(x,y) = \max\left\{d_\theta(x,y), \frac{d_\theta(x,fx)\, d_\theta(y,fy)}{1+d_\theta(fx,fy)}\right\}$ and
$N(x,y) = \min\{d_\theta(x,fx), d_\theta(x,fy), d_\theta(y,fx), d_\theta(y,fy)\}$
Then f has a unique fixed point.

Proof. Let $F(a,b) = \phi(a)$ by theorem 3.1 where $\phi: [0,\infty) \to [0,\infty)$ is continuous and
$\phi(0) = 0, \phi(b) < b$ where $b > 0$ and $\psi(b) = b$.
Thus, all the conditions of corollary 3.3 are satisfied. Hence, f has a unique fixed point.

Corollary 3.6, let (X,d_θ) be a complete b-metric space, and $f: X \to X$ be a self
Mapping. Suppose
$\theta(x,y)d_\theta(fx,fy) \leq \theta\big(M(x,y)\big) + LN(x,y)$
$\forall x,y \in X$ where $L \geq 0$, $\theta: [0,\infty) \to [0,\infty)$
is a continuous function such that
$\theta(0) = 0$ and $\theta(t) < t$ for $t > 0$ and
$M(x,y) = \max\left\{d_\theta(x,y), \frac{d_\theta(x,fx)\, d_\theta(y,fy)}{1+d_\theta(fx,fy)}\right\}$ and
$N(x,y) = \min\{d_\theta(x,fx), d_\theta(x,fy), d_\theta(y,fx), d_\theta(y,fy)\}$
Then f has a unique fixed point.

Proof. With choice $\theta(b) = lb, 0 < l < 1$.
Thus, all the conditions of corollary 3.5 are satisfied. Hence, f has a unique fixed point.

Example 3.7. Let $X = C([a,b]; R)$ be a real value function defined on $[a,b], f: X \to X$ where $f(x) = \frac{2x+5}{7}$ and define (X, d_θ) is an extended b metric space.
By $d_\theta(x,y) = \sup_{t\in[a,b]}|x(t) - y(t)|^2$ and
$\theta: X \times X \to [1,\infty)$ where
$\theta(x,y) = |x(t)| - |y(t)| + 2$.
So (X,d_θ) is a complete b-metric space. Thus

$$d_\theta(x,fx) = \sup_{t\in[a,b]}|x(t) - \frac{2x(t)+5}{7}|^2$$

$$= \sup_{t\in[a,b]}|\frac{6x(t)+5}{7}|^2$$

$$d_\theta(y,fy) = \sup_{t\in[a,b]}|y(t) - \frac{2y(t)+5}{7}|^2$$

$$= \sup_{t\in[a,b]}|\frac{6y(t)+5}{7}|^2$$

$$d_\theta(fx,fy) = \sup_{t\in[a,b]}|\frac{2x(t)+5}{7} - \frac{2y(t)+5}{7}|^2$$

$$= \sup_{t\in[a,b]}|\frac{6x(t)-2y(t)}{7}|^2$$

$$M(x,y) = \max\left\{d_\theta(x,y), \frac{d_\theta(x,fx)\, d_\theta(y,fy)}{1+d_\theta(fx,fy)}\right\}$$

$$= \max\left\{\sup_{t\in[a,b]}|x(t) - y(t)|^2, \frac{\sup_{t\in[a,b]}|x(t) - \frac{2x(t)+5}{7}|^2 \sup_{t\in[a,b]}|\frac{6y(t)+5}{7}|^2}{1+\sup_{t\in[a,b]}|\frac{6x(t)-2y(t)}{7}|^2}\right\}$$

$$= \sup_{t\in[a,b]}|x(t) - y(t)|^2.$$

Such that $\theta(x,y)d_\theta(fx,fy)$

$$= (|x(t)| - |y(t)| + 2)\sup_{t\in[a,b]}|\frac{2x(t)-2y(t)}{7}|^2$$

$$= 4(|x(t)| - |y(t)| + 2)\sup_{t\in[a,b]}|\frac{x(t)-y(t)}{7}|^2$$

$$\leq \frac{4}{49}(|x(t)| - |y(t)| + 2)\sup_{t\in[a,b]}|x(t) - y(t)|^2$$

$$\leq \frac{4}{49}d_\theta(x,y)M(x,y)$$

Thus, all the conditions of corollary 3.6 are satisfied. Hence, 1 is a unique fixed point of f.

CONCLUSIONS

This article presents the concept of C-class functions of the fixed theorem in incomplete extended b-metric spaces. We also prove that a fixed point of C-class functions exists in incomplete extended b-metric spaces. Further, some examples supporting the main results are provided. Our results extend and generalize corresponding results in the literature. The work presented provides a basis for researchers to work on in the future, and the work presented here is likely to provide a ground for the researchers to work in different structures by using these conditions.

ACKNOWLEDGEMENT

The first author was supported by Phetchabun Rajabhat University and Thailand Science Research and Innovation (Grant no. FRB640052/05).

REFERRENCES

1. Note on ϕ,ψ-contractive type mappings and related fixed point. The 2nd regional conference on mathematics and applications; 2014 Sep; Tehran, Iran; 2014.
2. Choudhury BS, Metiya N, Postolache M. A generalized weak contraction principle with applications to coupled coincidence point problems. Fixed Point Theory and Applications. 2013;152:1-21.
3. Boonwan C, Yamfang M, Thepa S, Sukchana T, Pruengam P, Pairintra R, et al. Development of a mathematical model to predict soil temperature for the growth of chrysanthemum sprouts. J Appl Res Sci Tech. 2020;19(1):74-85.
4. Bhaskar G, Lakshmikantham V. Fixed point theorems in partially ordered metric spaces and applications. Nonlinear Analysis. 2005;65 (7):1379-93.
5. Cortelazzo G, Mian G, Vezzi G, Zamperoni P. Trademark shapes description by string matching techniques. Pattern Recognition. 1994;27(8):1005-18.
6. Aydi H, Jellali M, Karapinar E. On fixed point results for alpha-implicit contractions in quasimetric spaces and consequences. Nonlinear Anal Model Control. 2016;21(1):40-56.
7. Bakhtin IA. The contraction mapping principle in almost metric spaces. Journal Of Functional Analysis. 1989;30:26-37.
8. McConnell R, Kwok R, Curlander J, Kober W, Pang S. ψ-S correlation and dynamic time warping: Two methods for tracking ice floes. IEEE Transactions on Geoscience and Remote Sensing. 1991;29:1004-12.
9. Czerwik S. Nonlinear set-valued contraction mappings in b-metric spaces. Atti Semin mat fis Univ Modena Reggio Emilia. 1998;46:263-76.
10. Abdeljawad T, Alzabut JO, Mukheimer A, Zaidan Y. Banach contraction principle for cyclical mappings on partial metric spaces. Fixed Point Theory A. 2012;154:1-7.
11. Abdeljawad T, Alzabut JO, Mukheimer A, Zaidan Y. Best proximity points for cyclical contraction mappings with boundedly compact decompositions. J Comput Anal Appl. 2013;15(4):678-85.
12. Kamran T, Ali MU, Postolache M, Ghiura A, Farheen M. Best proximity points for a new class of generalized proximal mappings. Int J Anal Appl. 2017;13(2):198-205.
13. Kamran T, Postolache M, Uddin F, Ali MU. Fixed point theorems on generalized metric space endowed with graph. J Nonlinear Sci Appl. 2016;9(6):4277-85.
14. Kamran T, Samreen M, Ain QU. A generalization of b-metric space and some fixed point theorems. Mathematics. 2017;5(2):19.
15. Suzuki T. A generalized Banach contraction principle that characterizes metric completeness. Proc Am Math Soc. 2008;136:1861-9.
16. Shatanawi W, Postolache M, Ansari AH, Kassab W. Common fixed points of dominating and weak annihilators in ordered metric spaces via C-class functions. J Math Anal. 2017;8(3):54-68.
17. Banach S. Sur les opérations dans les ensembles abstraits et leur application aux équations integrals. Fund Math. 1922;3:133-81.
18. Ansari AH, Razani A. Some fixed point theorems for C-class functions in b-metric spaces. Sahand Commum Math Anal. 2018;10(1):85-96.

DOI: 10.60101/jarst.2023.251308

Institute of Research and Development
Rajamangala University of Technology Thanyaburi

39 M.1 Klong 6, Thanyaburi, Pathumthani 12110, Thailand
Tel. (02) 549-4492 Fax. (02) 577-5038, (02) 549-4680

Website : https://ird.rmutt.ac.th

TCI
ศูนย์ดัชนีการอ้างอิงวารสารไทย
Thai-Journal Citation Index Centre

THAIJO